The dinosaurs that weren’t: osteohistology supports giant Ichthyosaur affinity of enigmatic large bone segments from the European Rhaetian (#89579)

First submission

Guidance from your Editor

Please submit by **2 Sep 2023** for the benefit of the authors (and your token reward) .

Structure and Criteria
Please read the 'Structure and Criteria' page for general guidance.

Raw data check
Review the raw data.

Image check
Check that figures and images have not been inappropriately manipulated.

If this article is published your review will be made public. You can choose whether to sign your review. If uploading a PDF please remove any identifiable information (if you want to remain anonymous).

Files
Download and review all files from the materials page.

12 Figure file(s)
2 Table file(s)
2 Other file(s)

Structure and Criteria

Structure your review

The review form is divided into 5 sections. Please consider these when composing your review:

1. **BASIC REPORTING**
2. **EXPERIMENTAL DESIGN**
3. **VALIDITY OF THE FINDINGS**
4. General comments
5. Confidential notes to the editor

You can also annotate this PDF and upload it as part of your review

When ready submit online.

Editorial Criteria

Use these criteria points to structure your review. The full detailed editorial criteria is on your guidance page.

BASIC REPORTING

- Clear, unambiguous, professional English language used throughout.
- Intro & background to show context. Literature well referenced & relevant.
- Structure conforms to PeerJ standards, discipline norm, or improved for clarity.
- Figures are relevant, high quality, well labelled & described.
- Raw data supplied (see PeerJ policy).

EXPERIMENTAL DESIGN

- Original primary research within Scope of the journal.
- Research question well defined, relevant & meaningful. It is stated how the research fills an identified knowledge gap.
- Rigorous investigation performed to a high technical & ethical standard.
- Methods described with sufficient detail & information to replicate.

VALIDITY OF THE FINDINGS

- Impact and novelty not assessed. *Meaningful* replication encouraged where rationale & benefit to literature is clearly stated.
- All underlying data have been provided; they are robust, statistically sound, & controlled.
- Conclusions are well stated, linked to original research question & limited to supporting results.

Standout reviewing tips

The best reviewers use these techniques

Tip	*Example*
Support criticisms with evidence from the text or from other sources	*Smith et al (J of Methodology, 2005, V3, pp 123) have shown that the analysis you use in Lines 241-250 is not the most appropriate for this situation. Please explain why you used this method.*
Give specific suggestions on how to improve the manuscript	*Your introduction needs more detail. I suggest that you improve the description at lines 57- 86 to provide more justification for your study (specifically, you should expand upon the knowledge gap being filled).*
Comment on language and grammar issues	*The English language should be improved to ensure that an international audience can clearly understand your text. Some examples where the language could be improved include lines 23, 77, 121, 128 – the current phrasing makes comprehension difficult. I suggest you have a colleague who is proficient in English and familiar with the subject matter review your manuscript, or contact a professional editing service.*
Organize by importance of the issues, and number your points	*1. Your most important issue* *2. The next most important item* *3. …* *4. The least important points*
Please provide constructive criticism, and avoid personal opinions	*I thank you for providing the raw data, however your supplemental files need more descriptive metadata identifiers to be useful to future readers. Although your results are compelling, the data analysis should be improved in the following ways: AA, BB, CC*
Comment on strengths (as well as weaknesses) of the manuscript	*I commend the authors for their extensive data set, compiled over many years of detailed fieldwork. In addition, the manuscript is clearly written in professional, unambiguous language. If there is a weakness, it is in the statistical analysis (as I have noted above) which should be improved upon before Acceptance.*

The dinosaurs that weren't: osteohistology supports giant Ichthyosaur affinity of enigmatic large bone segments from the European Rhaetian

Marcello Perillo [Corresp., 1], **Paul Martin Sander** [1, 2]

[1] Section Paleontology, Institute of Geosciences, Rheinische Friedrich-Wilhelms Universität Bonn, Bonn, Germany

[2] The Dinosaur Institute, Natural History Museum of Los Angeles County, Los Angeles, California, United States of America

Corresponding Author: Marcello Perillo
Email address: marcelloperillo.96@gmail.com

Very large unidentified elongate and rounded fossil bone segments of uncertain origin recovered from different Rhaetian (Late Triassic) fossil localities across Europe have been puzzling the paleontological community since the second half of the 19th century. Different hypotheses have been proposed regarding the nature of these fossils: giant amphibian bones, dinosaurian or other archosaurian long bone shafts, and giant ichthyosaurian jaw bone segments. We call the latter proposal the 'Giant Ichthyosaur Hypothesis' and test it using bone histology. In unidentified or putative ichthyosaur specimens from SW England (Lilstock), France (Autun), and Germany (Bonenburg), we consistently found a combination of common histological features: an unusual woven-parallel complex of longitudinal primary osteons, a novel bone tissue type, that we define as periosteal structural fiber tissue (PSFT), and a distinctive pattern of Haversian substitution in which secondary osteons often form inside primary ones. The splenial and surangular of the holotype of *Shastasaurus sikanniensis* from Canada were sampled for comparison. The results of the sampling indicate a common osteo-histology between all the specimens and a strong similarity to ossified tendons histology. A broad histological comparison is provided to reject alternative taxonomic affinities aside from ichthyosaurs of the very large bone segment. Most importantly, we highlight the occurrence of shared peculiar osteological processes in Late Triassic giant ichthyosaurs, reflecting special ossification strategies enabling fast growth and achievement of giant size and/or related to biomechanical properties akin to ossified tendons.

The dinosaurs that weren't: Osteohistology supports giant ichthyosaur affinity of enigmatic large bone segments from the European Rhaetian

Marcello Perillo[1], P. Martin Sander[1,2]

[1]Section Paleontology, Institute of Geosciences, University of Bonn, 53115 Bonn, Germany
[2]The Dinosaur Institute, Natural History Museum of Los Angeles County, Los Angeles, California 90007, USA.

Corresponding Author:
Marcello Perillo[1]
Martin-Görgens Str. 43, Bonn, North Rhine-Westphalia, 53117, Germany
Email address: marcelloperillo.96@gmail.com

Abstract

Very large unidentified elongate and rounded fossil bone segments of uncertain origin recovered from different Rhaetian (Late Triassic) fossil localities across Europe have been puzzling the paleontological community since the second half of the 19th century. Different hypotheses have been proposed regarding the nature of these fossils: giant amphibian bones, dinosaurian or other archosaurian long bone shafts, and giant ichthyosaurian jaw bone segments. We call the latter proposal the 'Giant Ichthyosaur Hypothesis' and test it using bone histology.

In unidentified or putative ichthyosaur specimens from SW England (Lilstock), France (Autun), and Germany (Bonenburg), we consistently found a combination of common histological features: an unusual woven-parallel complex of longitudinal primary osteons, a novel bone tissue type, that we define as periosteal structural fiber tissue (PSFT), and a distinctive pattern of Haversian substitution in which secondary osteons often form inside primary ones.

The splenial and surangular of the holotype of *Shastasaurus sikanniensis* from Canada were sampled for comparison. The results of the sampling indicate a common osteo-histology between all the specimens and a strong similarity to ossified tendons histology.

A broad histological comparison is provided to reject alternative taxonomic affinities aside from ichthyosaurs of the very large bone segment. Most importantly, we highlight the occurrence of shared peculiar osteological processes in Late Triassic giant ichthyosaurs, reflecting special ossification strategies enabling fast growth and achievement of giant size and/or related to biomechanical properties akin to ossified tendons.

Introduction

The Late Triassic covers an extremely long-time span (approximately 36 Ma), encompassing two of the fundamental biological revolutions of interest to paleontology, i.e., part of the Mesozoic Marine Revolution and the End-Triassic Mass Extinction. The Late Triassic also saw the rise of many tetrapod clades in the sea and on land that were to dominate the remainder of the Mesozoic (e.g., non-avian dinosaurs and plesiosaurs) and are still prominent today (e.g., birds, mammals). Nonetheless, the complex of biotic interactions of this Mesozoic Epoch and its protagonists still needs to be fully understood (Benton 2015; Kelley & Pyenson 2015). Giant ichthyosaurs (length>12 m), prominent elements of the ecological communities of Triassic seas, are no exception due to the absence of satisfactory fossils to unravel their evolutionary history and their still obscure extinction at the end of the Triassic Period (Sander *et al.* 2021).

Bone segments and putative giant ichthyosaurs from Europe

Large, but fragmentary bone finds from the famous Aust Cliff Rhaetic bonebeds of the Bristol area (southwestern UK) were already reported in the 19th century (Stutchbury 1850). These include what appeared to be large ~~leg~~ bone shafts of reptilian affinity leading to extensive

discussions in the paleontological community (Stutchbury 1850; Sanders 1876; Huene 1912; Storrs 1993, 1994; Benton & Spencer 1995; Naish & Martill 2008; Redelstorff, Sander & Galton 2014; Lomax *et al.* 2018). The Aust Cliff bonebed is one of a group of similar UK and continental European bonebed-type deposits formed in the Rhaetian epicontinental sea that covered much of Western and Central Europe (Barth *et al.* 2018; Cross *et al.* 2018; Perillo & Heijne 2023, Sander & Wellnitz, 2023, unpublished data) (Fig. 1). These bonebeds yield various tetrapod fossils of both, terrestrial and marine, origins, often showing fragmentary preservation (Storrs 1993, 1994). The proposed taxonomic affinities of the large to gigantic bone shaft, hereafter less suggestively called "bone segments", include labyrinthodonts (Stutchbury 1850), dinosaurs (Sanders 1876; Reynolds 1946; Storrs 1993, 1994; Benton & Spencer 1995; Galton 2005) and unidentified archosaurs (Redelstorff, Sander & Galton 2014).

The dinosaurian origin of said bone segments (hereafter 'Dinosaur Hypothesis') has been supported for the last decades, with Galton (2005) discussing the bone segments in detail and concluding that they either must represent sauropodomorph or, more likely stegosaur long bone shaft fragments (femur, ?tibia). Curiously, the material described by Galton also includes a transversely sectioned specimen (BRSMG Cb3870) of about the dimensions noted by Huene (1912). Galton did not cite Huene, and there is a possibility that the two authors did study the same specimen. Alternatively, more than one of the existing large bones in the Bristol collection were sectioned early on. Arguing against the identity of the two specimens is the poor preservation of the Galton specimen (whereas Huene emphasized the good preservation of his material) and the fit with another segment (whereas Huene noted the lack of fits).

Galton's conclusion as to the stegosaurian nature of the bone segments has since been questioned by multiple workers (Maidment *et al.* 2008; Naish & Martill 2008; Sander 2013; Redelstorff, Sander & Galton 2014; Lomax *et al.* 2018) due to the lack of diagnostic morphological features and stratigraphic arguments. In particular, the largest known stegosaur already occurring in the Late Triassic would be inconsistent with the known ornithischian fossil record and result in long ghost lineages (Galton 2005; Maidment *et al.* 2008; Naish & Martill 2008). Sauropods, on the other hand, would appear to be a reasonable option.

A histological test of sauropod affinities of the Aust Cliff bone segments was then conducted by Redelstorff, Sander & Galton (2014). Sampling two of the Aust Cliff specimens (BRSMG-Cb-3869 and BRSMG-Cb-3870, see Table 1), Redelstorff, Sander & Galton 2014 (2014) found a peculiar and previously undescribed set of histological characters (a thin cortex of fibrolamellar bone with longitudinal primary osteons and development of secondary osteons inside the primary ones), inconsistent with sauropod or other sauropodomorph affinities. In their primary cortex, sauropodomorph long bones show a different and rather uniform histology: laminar and plexiform fibrolamellar bone and, in the case of sauropods, almost no growth marks until late in life (Sander & Klein 2005; Klein & Sander 2007, 2008; Sander *et al.* 2011).

Following the recent find of a very large elongate bone segment (BRSMG Cg2488, 96 cm long) in the Rhaetian of Lilstock (Lomax *et al.* 2018), also in SW England, this segment and the Aust Cliff bone segments were identified as fragments of the surangular bones from giant

ichthyosaur jaws (Lomax *et al.* 2018). This interpretation by Lomax *et al.* (2018) was based on a morphological comparison with somewhat older giant ichthyosaurs from North America, specifically the Carnian *Shonisaurus popularis* from Nevada (Camp 1980) and the Norian *Shastasaurus sikanniensis* from British Columbia, Canada (Nicholls & Manabe 2004). We term this hypothesis of the affinity of the very large Aust Cliff bone segments the 'Giant Ichthyosaur Hypothesis'.

Support for the Giant Ichthyosaur Hypothesis would seem to come from an earlier find, now lost. Huene (1912) described a 1.4 m long bone segment from Aust Cliff which he identified as the fragment of a right lower jaw from a giant ichthyosaur, including part of four elements of the lower jaw (dentary, splenial, angular, surangular). Huene (1912) notes that this fossil had been accessioned to the "Bristol Museum" since 1877, presumably referring to today's Bristol City Museum and Art Gallery (BRSMG). However, since Huene's (1912) study, the specimen has not been mentioned again and it may well have been destroyed in WWII. According to Huene's (1912) description and illustration, the specimen consists of four non-fitting parts, the penultimate of which had been sectioned transversely at some earlier point in time before his study.

Similar finds to the Aust Cliff and Lilstock segments have come from the epicontinental French Rhaetian localities of the Autun area and from southern France (Fischer *et al.* 2014; Lomax *et al.* 2018) (Fig. 1), as well as most recently, from the German locality of Bonenburg (Sander *et al.* 2016; Wintrich *et al.* 2017) and the Swiss Alps (Sander *et al.* 2022, fig. s5). However, Fischer *et al.* (2014) did not extend their considerations to the UK material and did not cite Huene (1912). ~~Vice versa,~~ Huene just described this one specimen from Aust Cliff and did not comment on the putative dinosaur leg bone shafts from the same locality nor on the French Rhaetian ichthyosaur material, all of which was known at the time.

The Late Triassic giant ichthyosaur record

Ever since the work of Charles S. Camp in the Carnian Luning Formation of Nevada in the 1950s (Camp 1980), it has been clear that Late Triassic ichthyosaurs reached body lengths of 15 m or more and must have been substantially larger than post-Triassic ichthyosaurs. It is also now acknowledged that various other ichthyosaur finds from the Late Triassic must have reached over 10 meter in length aside from the most famous and complete *Shonisaurus popularis* from Berlin Ichthyosaur State Park in Nevada (Camp 1980; Kosch 1990; Hogler 1992; McGowan & Motani 1999, Kelley *et al.* 2022). Even larger and more complete than *S. popularis* is the holotype skeleton of *Shastasaurus sikanniensis* (Nicholls & Manabe 2004) from the middle Norian of British Columbia, Canada. Based on field data, this individual is estimated to have been 21 m long (Nicholls & Manabe 2004).

Most giant ichthyosaurs are represented by woefully incomplete, disarticulated and fragmentary material from around the world (Camp 1976; Callaway & Massare 1989; McGowan & Motani 1999; Sander *et al.* 2022; Kelley *et al.* 2022) which hinders the anatomical descriptive effort. In continental Europe, these fragmentary, often reworked, and unresolved finds attributed

to giant ichthyosaurs come from late Norian to Rhaetian outcrops of France (Fischer *et al.* 2014), the eastern Swiss Alps (Sander *et al.* 2022) and from a recently discovered Aust Cliff-type bonebed near the central German village of Bonenburg (Fig. 1) (Sander *et al.* 2016; Wintrich *et al.* 2017). Unlike all the other Rhaetian localities with putative giant ichthyosaurs, the Bonenburg deposit is precisely dated palynologically ranging from late middle to early late Rhaetian in age (Schobben *et al.* 2019; Gravendyck *et al.* 2020). The Bonenburg ichthyosaur fossils include large but very short vertebral centra, a very large neural arch, and very large rib fragments (Sander *et al.* 2016; Witkowski, 2017, unpublished data; Lammsfuß, 2022, unpublished data). In addition, the bonebed frequently yields heavily abraded fragments of thick cortical bone up to 25 cm in length (Fig. S3A, S5A), which we hypothesize to be fragments to the more complete British and French bone segments (Fig. S1A).

Understanding the affinity of the fragmentary Late Triassic ichthyosaurs and of the large, more obscure fragmentary finds, is important because of the absolute size of the remains, representing records of the largest animals inhabiting the Late Triassic oceans (Lomax *et al.* 2018; Sander *et al.* 2022), far exceeding in size of any other marine tetrapods except for the largest species of baleen whales and archaeocetes (Bianucci *et al.* 2023).

The lack of clear and unequivocal external morphological features in the Rhaetian European bone segments due to their fragmentary and reworked nature makes alternative approaches such as microstructure analysis (microanatomy and osteohistology) critically important in investigating the possible affinities of these fossils. Both Galton (2005) and Lomax *et al.* (2018) illustrated cross sections of UK fossils and discussed microanatomy (but not histology, which is not accessible without thin-sectioning). Galton compared the midshaft microanatomy of BRSMG 3469, 3470, and 4063 from Aust Cliff to that of various dinosaurs and concluded that the fossils must represent stegosaurs because of the coarse cancellous bone structure of the medullary region. Lomax *et al.* (2018) noted and illustrated in detail the same coarse cancellous bone structure but did not use microanatomical arguments as evidence for determining affinity, only cross-sectional shape. Histological analysis was already performed on two Aust Cliff specimens (BRSMG-Cb-3869 and BRSMG-Cb-3870) by Redelstorff, Sander & Galton (2014) (Table 1), but without considering possible ichthyosaurian affinities of the fossils. Instead, Redelstorff, Sander & Galton (2014) adhered to the paradigm that the Aust Cliff segments were shafts of dinosaur long bones.

Here we undertake a detailed and comprehensive comparison and sampling of most European “mystery bone” specimens for histological analysis. The main aim of this study thus is to histologically test the Giant Ichthyosaur Hypothesis by recording shared histological characters among European material of confirmed or proposed ichthyosaurian nature, on one hand, and bonafide Late Triassic giant ichthyosaurs, such as *S. sikanniensis*, on the other. We also compare the “mystery bone” histology with other terrestrial and aquatic tetrapods known have reached very large body size in the Late Triassic such as sauropodomorph dinosaurs, rauisuchians, dicynodonts, and plesiosaurs.

Materials & Methods

Materials

The material used in this study consists of bone histological samples taken from various specimens borrowed from multiple institutions as listed in Table 1. In summary, there are eight sets of samples (Table 1) including skull and mainly lower jaw elements (Figs S1, S2, S3, S4, S5). These include two samples (surangular, splenial) from the *S. sikanniensis* holotype (Nicholls & Manabe 2004) (Fig. S2), one sample of the Lilstock putative ichthyosaur surangular (Lomax *et al.* 2018), three samples of "dinosaur bone shafts" reinterpreted as giant ichthyosaur surangular segments from the Aust Cliff Rhaetic bonebed (Galton 2005; Redelstorff, Sander & Galton 2014; Lomax *et al.* 2018), two samples from a giant putative ichthyosaurian lower jaw (Fischer *et al.* 2014), specifically the surangular (Lomax *et al.* 2018), from Autun, France (Fig. S1), and finally 16 cortex fragments of various sizes from Bonenburg, Germany (Figs S3, S4A, S5A). For details on all of these samples, including sampling locations and methods, and their current identification, see Supplemental Article S1.

The thin sections used for the study are either in the paleohistological collections of the IGPB or with the sampled fossils (see Table 1). Note that two of the Aust Cliff thin sections were already studied by Redelstorff, Sander & Galton (2014).

Methods

Thin sections

Except for the *S. sikanniensis* holotype, jaw bones and putative jaw bones were sampled by core drilling, following Sander (2000) and Stein & Sander (2009) (Table 1). The *S. sikanniensis* lower jaw was sampled with a Dremel-type cutting tool, making two parallel cuts spaced 18 mm apart and then preparing out the sample. Complete cross sections and longitudinal sections were obtained from smaller specimens of cortical bone fragments from Bonenburg by cutting with a rock saw after embedding with a protective epoxy putty. Cores and full sections were then processed into thin sections following Lamm (2013), with slight modification of the standard technique: wet silicon carbide powder of grit sizes of 600 and 800 was used for the grinding and polishing processes.

Once covered, the thin sections were studied under a Leica DMLP light microscope in regular illumination and by using cross-polarization and circular polarization techniques. Circular polarization (Bromage *et al.* 2003) was obtained through the use of a pair of commercially available polarizing glasses for 3D movie viewing to replace the polarizer and the analyzer of the microscope. This allows observation of the thin sections in circular polarized light without the Maltese cross effect. Photomicrographs were taken using a Leica DFC420 camera (software Leica Firecam, ver. 3.1, 2007, © Leica Microsystems, Switzerland, Ltd), a Dino-Eye camera (software DinoCapture 2.0 ver 1.5.45 © 2016 AnMo Electronics Corporation),

and with a Canon EOS2000D (software EOS Utility ver. 3.16.11, 2023, © Canon Europa N.V. and Canon Europe Ltd 2002-2009) mounted on the microscope.

Terminology, including new terminology

Histological terminology follows Buffrénil & Quilhac (2021a) for general osteohistology, Scheyer & Sander (2004) for the structural fibers concept, and Buffrénil & Quilhac (2021b) for secondary osteon features. An important feature in this category are concentric osteons, most recently discussed by Buffrénil & Quilhac (2021b). In these, a secondary osteon develops inside a Haversian canal, i.e., inside a preexisting secondary osteon (Lacroix 1970). Concentric osteons are not to be confused with double-zoned secondary osteons (Skedros, Sorenson & Jenson 2007) where the centripetal infill of a secondary osteon happens in stages, but without intervening resorption (Skedros, Sorenson & Jenson 2007). We did not observe such double-zoned secondary osteons in this study, however. Importantly, neither of these terms describes the situation observed already by Redelstorff, Sander & Galton (2014), in which a secondary osteon develops inside a primary one. We refrain from erecting new terminology for this situation but use a simple descriptive approach.

Nevertheless, the histology of the giant ichthyosaur material is so unusual in another feature that does require new terminology. This new terminology was coined to aid in the description of a novel histology in primary bone of periosteal origin for which no proper definition was found in the literature. This new term is 'periosteal structural fiber tissue' or PSFT.

The term is briefly defined here, but the detailed description is found in the Results section. PFST is a feature at the bone tissue level of integration and thus is to be used in conjunction with 'lamellar bone tissue', 'woven-parallel complex', 'Haversian tissue', etc. (Buffrénil & Quilhac 2021a, b). In fact, PSFT is one of the 'woven-parallel complexes with longitudinal osteons' of Buffrénil & Quilhac 2021a). The 'woven' part of the complex is similar to the interwoven structural fibers (Scheyer & Sander 2004) of metaplastic origin seen in osteoderms and ossified tendons (e.g., Scheyer & Sander 2004; Klein, Christian & Sander 2012, Horner, Woodward & Bailleul 2016, Surmik *et al.* 2023). However, PSFT is of periosteal origin and the structural fibers are set in an isotropic matrix (Figs 2A, B, 5B, C). The 'parallel' part of the complex is developed as strictly longitudinal primary osteons. We would like to emphasize that the term is mainly for descriptive purposes in this study, and we do not ~~really~~ understand the osteogenic processes behind it. We are also ~~not sure~~ how widespread the tissue may be among amniotes ~~in general~~.

The general histological description follows the 3-Front Model of Mitchell & Sander (2014) (Fig.3) in which the osteohistological pattern observed in an amniote cortical bone sample is conceptualized as being generated by the successive outward advance of three fronts and their speed. These fronts are the apposition front (where bone tissue is formed), followed by the Haversian substitution front (where primary bone tissue is replaced by secondary tissue), and the resorption front (where bone tissue is resorbed to make space for bone marrow). Due to the

undefined taxonomical state of the specimens and lack of clear homology in sample location (aside for BRSMG-Cb-3869 and BRSMG-Cg-2488 R-101), the model is only used for descriptive purposes and general comparison, but not for define relative developmental stages.

Porosity quantification

Sections were scanned with a flatbed scanner or photographed at the microscope with a cell phone camera. In the latter case, successive microphotos were merged using the photomerge tool in Photoshop (Ver 20.0.4 20190227.r.76). Both scans and merged photos were transformed into binary pictures for porosity quantification (Fig. S6). Porosity quantification was executed with the software BW-counter © Peter Göddertz, IGPB). Porosity is expressed as the percentage of white area (vascular and trabecular cavities) vs. black area (mineralized bone material).

Results

Shared histology of the British and French samples

General histological and microanatomical description

The outer cortex, laid down by the apposition front, of all European putative jaw bone samples is generally characterized by dense primary tissue organized in wavy growth cycles of PSFT (Fig. 2A, 3) (for definition of PSFT see Terminology, for detailed description see section -PSFT with longitudinal vascular canals- below). Vascularization is characterized by longitudinal vascular canals (Fig. 3). Immature primary osteons and vascular canals open up to the periosteal surface, building up an ornamented wavy surface (Figs 3, 4B) in the sections. On the bone surface, this histology correlates with distinctive longitudinal striations, nicely illustrated by Lomax *et al.* (2018, fig. 4). Vascular canals and primary osteons are arranged in circumferential rows demarcated by closely spaced skeletal growth marks (SGM, we do not imply that they are annual, however, see Discussion) that vary in number (Figs 2A, 3, 4A, B). SGM appear as depositional layers of primary bone. They vary in thickness and show alternating light-dark coloration and surround superficial periosteal vascular canals (Figs 2A, 4A, B). The differential coloration seems to be related to differences in PSF density and orientation. Vascularization as observed in longitudinal sections does not show anastomoses between vessels, with vessel cross sections rarely showing shapes more complex than an elongated ellipsoid (Fig. 4C).

The Haversian substitution front is diffuse in that the outer cortex shows scattered evidence of secondary remodeling through small resorption cavities and secondary osteons inside primary ones (Fig. 2A, D), or even mature secondary osteons (Fig. 4A). The deep cortex, which is fully within the Haversian substitution front, can again be subdivided in an outer ‘templating’ deep cortex (tDC) and an inner, completely remodeled area, where none of the primary pattern of vascularity is preserved (Fig. 3). This pattern was already described in detail by Redelstorff, Sander & Galton (2014, fig. 4). However, the thickness of these two subzones of deep cortex varies between samples (Fig. 3).

The 'templating' deep cortex is so named because it preserves most or some of the original primary vascular architecture (Figs 3, 4D). This is because of the peculiar pattern that Haversian substitution is initiated from existing primary vascular canals, resulting in a ~~dominance~~ of secondary osteons inside primary ones. The primary osteons thus clearly influence the course of the secondary ones, even leading to rows of exclusively secondary osteons forming complete Haversian tissue, ~~templating~~ the primary rows. Appositional rows of primary osteons may be followed ~~or preceded~~ by rows of secondary osteons inside secondary ones, i.e, concentric osteons (Fig. 2A, D). Deeper into the cortex, and thus further inward from the Haversian substitution front, there are only concentric osteons.

Osteons have a high number of lamellae and a small vascular canal, which results in a rather low porosity between 17% and 13% (Fig. S6 A-E), possibly indicating an osteosclerotic state of the cortex. The templating we observe is different from normal Haversian substitution in amniotes in which the cutting cones of secondary osteons show little regard for preexisting structures.

Different osteon layers can also be characterized by oval osteon cross sections in which the long axis of the oval is parallel to the outer bone surface alternating with osteons with more radially oriented long axes of their cross sections. Osteon cross sections vary consistently between circumferential rows (Figs 3, 4E), possibly indicating variations in growth rate (Woodward 2019). Migratory and incipient osteons (Skedros *et al.* 2007; Mitchell 2017) are present, but concentric ones represent the majority of osteons in the "templating" cortex.

Further inward from the "templating cortex", the regular deep cortex can be seen as resulting from complete secondary reconstruction (Fig. 3). This part of the cortex is characterized by more chaotic secondary osteons that have obliterated the primary vascular architecture by several cycles of secondary osteon formation. The result is normal Haversian tissue which marks the full effect of the Haversian substitution front (e.g. Fig. 3D).

The boundary of the perimedullary region, i.e., the resorption front, is also diffuse (Fig. 3). Here, the deep cortex becomes more and more affected by larger resorption cavities lined only by a few lamellae. Porosity in the perimedullary region is between 65 to 85% (Fig. S6 A-E). This signifies an increasing imbalance between secondary bone deposition and resorption activity and initiates the formation of secondary trabeculae (Fig. 3). Through the activity of the resorption front, the perimedullary region is rich in resorption cavities replacing bone tissue with some secondary osteons and transitioning to a medullary area of secondary trabecular bone (Fig. 3).

In cases, where the resorption front has overtaken the Haversian substitution front, interstitial areas of primary tissue consisting of PSFT are visible (Fig. 4) between the secondary trabeculae. The percentage of interstitial primary tissue decreases inwards but is patchy. As noted, the resorption front is irregular and not developed as a clear endosteal resorption front (Fig. 3). Our histological observations are consistent with the descriptions and illustrations of cross-sectional microanatomy given by Galton (2005), Fischer *et al.* (2014), and Lomax *et al.* (2018), who all note that there is only a very small open medullary cavity surrounded by an extensive zone of inward-decreasing trabecular density (Galton 2005, figs 4-6; Fischer *et al.*

2014, fig. s5; Lomax *et al.* 2018, fig. 6). Fischer *et al.* (2014, fig. s5) interpret this open medullary cavity as the dental groove, however.

Both the largest Aust Cliff bone segments (BRSMG Cb 3869) and the Lilstock specimen show conspicuous cavities in the thin sections (Fig. 3). There are two well identifiable in the latter and one clearly identifiable and a tentatively second one in the former (Figs 3, S6A, C). Based on the sampling location, these open cavities represent the nutrient canals extending inwards from the elongate foramen opening in caudal direction (already described by Huene 1912 and identified as the fossa surangularis by Lomax *et al.* 2018) on the bone surface. On the outward margins of the cavities (those facing the periosteal surface), both samples show primary tissue characterized by skeletal growth marks (Fig. 4E, F). These marks are not parallel to the outer surface of the bone but to the rim of the cavities, indicating centripetal bone apposition into the cavity. This way, the cavities can be identified as representing the nutrient canals: both samples show signs of resorption along the inner and lateral margins of the cavities, indicating microanatomical drift related to the growth of the bone enclosing the canal.

'Templating' remodeling and secondary osteons inside primary ones

As noted, the distinctive 'templating' secondary remodeling is shared between all samples (Table 2). Among the material in question, secondary osteons inside primary ones were first observed in Aust Cliff samples BRSMG-Cb-3869 and 3870 by Redelstorff, Sander & Galton (2014). It is possible to identify secondary osteons inside primary ones through the method adopted by Redelstorff, Sander & Galton (2014), i.e., focusing through the sample in normal light, using higher magnifications, a nearly closed diaphragm, and the condensor, or by observing the position of the resorption/cementing lines through the λ filter. The occurrence of multiple generations of secondary osteons inside primary ones (Fig. 2A, D) tends to maintain the original periosteal appositional rows (Fig. 3) as noted above. Secondary osteons inside primary ones signal the advancing Haversian substitution front, and may occur quite closely to the outer bone surface in the outermost cortical layers. Whereas secondary osteons inside primary ones also have been reported in mammals (e.g., Sander & Andrassy 2006 and the reference cited above), in these, they are not such a consistent feature as observed in the templating cortex of our specimens.

PSFT with longitudinal vascular canals

All European Rhaetian putative jaw bone samples share the same primary bone type (Table 2): an unusual woven-parallel complex with highly ordered longitudinal primary vascularization and periosteal structural fiber tissue, PFST. Whereas in PSFT, the parallel component of the woven-parallel complex is represented by typical osteonal lamellar bone of the longitudinal primary osteons, the unusual character is its woven component, building up the scaffold of the bone (Fig. 2 A-C).

PSFT is a type of woven-parallel complex because it is a combination of coarse mineralized structural collagen fibers and of a matrix of isotropic woven bone (Stein & Prondvai

2014, Buffrénil & Quilhac 2021a) (Fig. 2B). Under cross-polarized light in cross sections, PSFT is easily identifiable by the presence of a birefringent network of structural fibers with rectangular or hexagonal cross sections (Fig. 2B). The structural fibers networks are characterized by high brightness and appear conspicuous against the dark matrix of woven bone (Fig. 2B). The width and length of the structural fibers is variable, and strands intertwine with each other, overlapping in a fabric-weave pattern, forming 60° to 90° angles with each other and a 30° angle with the outer bone surface. Under the λ-filter, the fibers oriented in one direction take a bluish or greenish color (the latter if the section is too thick), opposed to a yellowish or dark orange (if the section is too thick) of the opposite ones, switching between these two colors with stage rotation, showing birefringence in a similar fashion to what happens to differently oriented lamellae lining vascular cavities (Fig. 2C). Circular polarization reveals the true arrangement of these fibers to be circular and coiled (Fig. 2C). The rectangular and hexagonal shape seen in crossed polarizers is therefore revealed to be an artifact, resulting from the Maltese-cross effect. The PSFT shows heterogeneity in brightness. The areas of denser fibers clustering are often correlated with lower brightness under cross-polarized light, both in longitudinal and cross sections (Fig. 2E).

In longitudinal section, PFST is characterized by parallel bundles of short fibers. These extend through the surface following the direction and angles of the vascular canals (Fig. 2E). The fibers appear as black scars in the tissue and show no birefringence, similar to osteocyte lacunae and canaliculi; this indicates a non-mineralized state of these structures. The fibers can be arranged in bundles of differently oriented units, intertwining with each other at different angles, from acute to orthogonal (Fig. 2E).

Osteocyte lacunae are extremely numerous in the areas with PSFT, showing a wide variety of shapes from irregular plump to discoidal flattened. The distribution of osteocyte lacunae is generally irregular without any apparent relation to other histological features. Lacunae are very dense in some areas while nearly absent in others. These dense irregular osteocyte lacunae are left by multipolar static osteocytes as is typical for a woven-parallel complex (Stein & Prondvai 2014, Buffrénil & Quilhac 2021a). Osteocytes tend to form chaotic clusters where strands and bundles of non-mineralized fibers are present (Fig. 2E). The number of osteocyte lacunae is high in the primary osteons as well, centripetally increasing in density from the border of the vascular opening toward the center of the primary osteon. Given the variability in shape and size both of the lacunae and of their canaliculi (sometimes apparent, sometimes not visible), it is likely that the more spindle shaped osteocytes lacunae found in the primary matrix represent fibrocytes.

Shastasaurus sikanniensis **holotype jaw bone samples**

Both of the jaw bone samples from the holotype of *S. sikannisenis* show poor preservation, which hides most of the discernable features in the areas where bone is most altered. This is particularly evident in the surangular. Poor preservation of birefringence is accompanied by a dark brown stain of the tissue, making it nearly opaque. However, with sufficiently bright illumination, the salient features, in particular the presence of PSFT, can be discerned (Fig. 5B-

D). Both the surangular and splenial histology are characterized by highly spongious bone (respective porosity ~ 82% and ~ 60%) constituted by a large area of secondary trabecular bone, dark brown in color under the crossed polarizers (Fig. 5B). Towards the outer bone surface, which appears to be compromised by preparation (see below), there are interstitial areas of primary tissue characterized by distinctive PSFT, with an outwards increase in frequency. Although no obvious dense cortical bone is present, a decrease in porosity is detectable toward the outer bone surface of both specimens (respectively 64% and 43% porosity) with small vascular longitudinal cavities and higher compactness. The vascularization, consisting of large Haversian canals and resorption cavities, is longitudinal (Figs 5, S6E, F). The secondary osteons visible present only few ~~layers of~~ centripetal lamellae. On the outer bone surface, the presence of osteons half cut open indicates the removal of tissue due to taphonomic or diagenetic causes or harsh preparation (Fig. 5A). However, the bone tissue is never sufficiently compact to not determine if there would have been secondary osteons inside primary ones.

Indeterminate cortical fragments from Bonenburg, Germany

The largest cortical fragment from Bonenburg (WMNM P88133) has a primary cortex rather similar to the previously discussed samples from Europe. However, observation of histology of ~~it~~ and most of the other Bonenburg samples is hampered by a nearly opaque outer diagenetic zone >2 mm wide that makes it ~~sometimes~~ difficult to observe the histology ~~right~~ below the outer bone surface (Fig. 6A, B). The remaining bone tissue is very well ~~preserved, however.~~

As in the other specimens, vascularization is strictly longitudinal (Fig. 6A, B). Simple vascular canals and primary osteons are arranged in surface-parallel rows which may be enhanced by SGM hugging the vascular canals (Fig. 6B). An ~~EFS~~ does not appear to be ~~developed~~. The bone tissue, in which the vascular canals and primary osteons are set, consists of PSFT (Fig. 6C).

The SGM show alternations of differently colored matrix but do not show an appreciable pattern in width differences, while they appear to show differences in fiber density. Under cross-polarized light, it is possible to observe clearly bright coarse fibers in the paler yellow areas, with a reduction of their presence corresponding with increased darkness in areas of darker brown color (Fig. 6B, C, S4C, D). The darkest skeletal growth marks seem to be constituted only by the amorphous isotropic matrix and show no presence of structural fibers (Fig. 6C).

Osteocyte lacunae are numerous in the PSFT with mainly plump and irregularly shaped ones throughout tissue, while more flattened ones are scarcer and present only in centripetal lamellae of osteons (Fig. 6D). Osteocyte lacunar density and size is greater in the primary bone matrix compared to the lamellar bone of osteons (Fig. 6D).

The largest fragment WMNM P88133 is characterized by a continuous gradient in bone compactness from the inner more cancellous area to the outermost cortex (Fig. 6A), resulting from the advancement of the Haversian substitution and resorption fronts. A wide and diffuse "non-conservative" Haversian substitution front is detectable toward the center of the section,

evidenced by the interruption of the continuity of semicircular SGM (Fig. 6B). Elsewhere in the section, secondary osteons develop preferentially inside primary ones, conserving the primary arrangement of the osteon rows (Fig. 6B, C). Rarely, there are secondary and primary osteons showing, ~~centripetally to the resorption line,~~ layers of anisotropic woven bone (Fig. 6D) alongside osteons showing presence of fibers similar to the ones of the surrounding matrix of PSFT.

In the deep cortical area, there is a high amount of resorption cavities eroded into the compact bone which consist of primary bone only partially replaced by secondary remodeling. Resorption cavities are lined by lamellar bone resulting in an increasingly cancellous condition.

The histological picture of the longitudinal section (Fig. 6E) is consistent with that of the cross section. The longitudinal section is dominated by simple longitudinal canals with a very limited degree of anastomosis. When adding the λ-filter, it is possible to observe diffuse presence of strands of thin, dark fibers of variable length, distributed mainly longitudinally (Fig. 6E). Sometimes, the fibers intersect each other next to the edges of the vascular openings (Fig. 6E). The borders of secondary osteons are lined by bright lamellar bone, darker bone tissue, and by both types together in an alternating fashion.

The thin sections produced from WMNM P-uncatalogued and the numerous smaller unidentified cortical fragments all show the same primary bone tissue as the largest one and overall general features that were described previously (Fig. S4, S5). While the larger WMNM P-uncatalogued could be derived from cranial material, like WMNM, no precise anatomical placement is possible for the smaller fragments in the context considered.

Discussion

Rejection of the "Dinosaur Hypothesis" and of other non-ichthyosaurian amniotes

Although we do not question the ichthyosaur status of the larger specimens based on their morphology (Fisher *et al.* 2014, Lomax *et al.* 2018), the morphological information provided by the more fragmentary specimens (BRSMG-Cb-3869, BRSMG-Cb-3870, BRSMG-Cb-4063 and WMNM P88133) may be considered insufficient for recognizing their systematic affinities, and a comprehensive histological comparison is needed. Based on the histological evidence obtained from sampling bonafide (i.e., *S. sikanniensis*) and putative Late Triassic giant ichthyosaurs, we regard as relevant four histological features (Table 2), three of which had already been noted by Redelstorff, Sander & Galton (2014) in a study of more limited scope aimed at testing the "Dinosaur Hypothesis" but not the "Giant Ichthyosaur Hypothesis".

These four features are: 1) PSFT (overlooked by Redelstorff, Sander & Galton 2014), 2) strictly longitudinal vascular architecture, 3) closely spaced skeletal growth marks structuring primary osteons and vascular canals (SGM), and 4) abundance of secondary osteons inside primary ones. Whereas PSFT on its own and also secondary osteons inside primary ones have only rarely been observed in amniotes before, the combination of all four features is unique to the material sampled here, and even small fragments of long and skull bone cortex are diagnostic for

giant ichthyosaurs. The occurrence of such a specific combination is possibly a powerful tool that can be used for reliable identification of cortical bone segments as pertaining to giant ichthyosaurs, consistent with the scanty morphological evidence.

To test for the presence of a similar combination of traits and to further test the "Giant Ichthyosaur Hypothesis", we underwent an extensive histological comparison considering a "Dinosaur Hypothesis", involving Sauropodomorpha and Stegosauria and a "Non-dinosaurian Hypothesis", involving known large sized or giant Late Triassic tetrapods, terrestrial and aquatic. The results of this comparison are summarized in Table 2 and more extensively discussed in Supplemental Article S2. We found that the uniqueness of the combination of histological features of the fragments (Table 2) paired with their large size allows for no convincing support for affinities to alternative coeval giant tetrapods, dinosaurian or non-dinosaurian.

Possible analogs and the nature of PSFT

Although PSFT has not been explicitly described in the literature, it is not uncommon to see published micrographs showing this type of matrix or apparently similar ones. A brief, but probably not complete, list of examples suggests the presence of PSFT in a wide variety of amniotes: in a rib of a large *Nothosaurus* specimen (Klein, Canoville & Houssaye 2019, fig. 4n, o), in the humerus of the ornithopod dinosaur *Telmatosaurus* (Buffrénil & Quilhac 2021a, fig. 8.6a), and in a rib of the thalattosuchian crocodylomorph *Metriorhynchus* (Buffrénil, Quilhac & Cubo 2021 fig. 10.2f).

Coarse crossed mineralized fibers similar to those observed in our samples are often referred to as interwoven structural fibers (ISF) and are characteristic of ossified tendons and osteoderms, usually associated with metaplastic ossification (Organ & Adams 2005; Klein, Christian & Sander 2012; Vickaryous, Meldrum & Russell 2015; Scheyer Syromyatnikova & Danilov 2017; Buffrénil & Quilhac 2021a fig. 8.7h; Surmik *et al.* 2023). It is important to note that the developmental nature of metaplastic bones is yet to be fully understood and that "metaplasia" can encompass a variety of different cellular mechanisms (Horner, Woodward & Bailleul 2016; Buffrénil & Zylberberg 2021). Furthermore metaplastic bone can occur in combination with other more common bone types such as periosteal bone (Organ & Adams 2005; Surmijk *et al.* 2023).

Several histological studies of non-amniote tetrapods show the presence of structural fibers as well, both in cranial bone cortices of metoposaurid temnospondyl *Metoposaurus* (Gruntmejer, Konietzko-Meier & Bodzioch 2016; Gruntmejer, Bodzioch & Konietzko-Meier. 2021) and in the humerus periosteal cortex of an indeterminate cyclotosaurian temnospondyl (Konietzko-Meier *et al.* 2019 fig. 3g). While the latter study does not address the developmental origin of such structures (only mentioning them as coarse fibers), the former describe them as ISF and present them as proof of metaplastic developmental process being involved in the formation of dermatocranial bones of dermal origin.

As noted, PSFT remarkably resembles ISF networks seen in metaplastic bone tissue of osteoderms (Scheyer & Sander 2004) and longitudinal crossed fibrils of ossified tendons of various tetrapods. However, we introduced the new term in order to set this clearly periosteal

tissue apart from metaplastic tissues. Nevertheless the similarity of PSFT with metaplastic bone tissue is remarkable, suggesting a shared osteogenetic process. Horner, Woodward & Bailleul (2016) proposed metaplastic mineralization to be distinguished from periosteal bone by the lack of true Haversian remodeling and osteocyte lacunae. However, for the purpose of our comparison, we disagree with this statement, in agreement with Organ & Adams (2005), Surmik *et al.* (2023) and with our personal observations on ossified tendons stored in the GIPB histological collection.

Aside from the clear similarity between PSFT and longitudinal crossed fibers, our samples and ossified tendons share longitudinal strands of unmineralized fibers in a herringbone pattern (Figs 2E, 4C, 6E, S6C.), the presence of numerous irregular, spindle-shaped cellular lacunae identifiable as fibrocytes, and presence of fibers or poorly mineralized tissue in endosteal osteon bone. Therefore, the presence of endosteal fibrous bone, and not lamellar, represent another similarity between our samples and metaplastic bone. The SGM we describe for the specimens find strict similarity with the structures reported by Horner, Woodward & Bailleul (2016) as zones of varying primary orientation and density of the fibers (Horner, Woodward & Bailleul 2016 fig. 2d-f). We find that the hypothesis proposed by Horner, Woodward & Bailleul (2016), following which, the variable color of similar structures is to relate to density and orientation of the fibers observable in longitudinal sections in ossified tendons, fits our observations (Fig. S5C, D), explaining the appearance of such marks. Contrasting to what reported by Horner, Woodward & Bailleul (2016) for ossified tendons, the SGM are identifiable as classical cycles of periosteal apposition, given the clear primary development of these structures in relation to the spatial distribution of periosteal canals and nutritional foramina, and the presence of osteocyte lacunae.

Finally, the question arises if the bone tissue with PSFT described in this study may be viewed as an apomorphy of a clade of giant ichthyosaurs. This would have to be tested by phylogenetic analysis incorporating histological characters, which may well find PFST as a non-unique synapomorphy.

Templating remodeling driven by unmineralized fibrous matrices

The phenomenon of "templating" remodeling, as a diffuse process of spatial development of bone remodeling units ~~(BMU) l~~ matching the position of pre-existing primary or secondary osteons, has been reported for different bones in multiple aquatic taxa such as lower jaws ichthyosaurs (this study), long bones in plesiosaurs (Sander & Wintrich 2021) and temnospondyls (Konietzko-Meyer *et al.* 2019). Furthermore, Surmijk *et al.* (2023) reported the presence of concentric osteons in ossified tendons. The occurrence of a shared unusual feature in the formation of highly different bone ~~development~~ (e.g. periosteal of lower jaws and long bones vs metaplastic of ossified tendons and osteoderms), hints at a common osteogenic process which has received limited attention in the literature. Most of these bones exhibit a matrix composed of both coarse mineralized and unmineralized fibers, although there are currently no published reports on plesiosaurs. In the process of bone resorption, osteoclasts are unable to act on the mineral bone matrix until the organic protective layer of bone lining cells is removed by cambial cells

(Zylberberg 2021). It is also hypothesized that sites characterized by non-mineralized structures are less attractive or accessible to osteoclasts (Aaron 1980; Jones, Boyde & Ali 1984; Aaron 2012). The widespread presence of non-mineralized fibers may significantly inhibit the progression of BMUs in highly fibrous bone matrices, resulting in preferential areas of osteoclast activity in osteon lamellar bone, poorer in unmineralized elements. The presence of a matrix richer in unmineralized fibers may induce primary osteons to serve as preferential 'highways' for osteoclast activity, particularly during the initial resorptive phases, thus explaining the occurrence of diffuse 'templating' remodeling.

Alternatively, a difference between the regulatory signals originating from the osteocytes in the outer cortical matrix and those within the osteon bone may be the primary driving force behind osteoclast regulation and attraction. The regulatory activity of osteocytes is known to be influenced by mechanical loading during development, and it appears to vary based on lacunar shape (van Oers, Wang & Bacabac 2015). Therefore, it is plausible that the numerous and highly heterogeneous lacunar spaces observed in the matrix might have played a crucial additional role.

Implications of PSFT for growth rate, giantism and feeding behaviour

Several features we described are commonly associated with fast growth rates, the most standard being a histology dominated by PWC, high vascularization rate, high remodeling rate with multiple generation osteons and high amounts of osteocytes lacunae, both irregular and spindle shaped (Buffrénil & Quilhac 2021b). The presence of numerous open canals in the outer cortex indicates an active growth stage for all the sampled bones and a well-vascularized external periosteal surface. The presence of unmineralized fibers in the cortex could be related to a rapid mineralization of the osteoid layers laid down by the periosteum as well to the occurrence of fibrocytes (Buffrénil & Quilhac *et al.* 2021a). The occasional presence of woven bone as endosteal infilling of osteons may be another feature supporting fast bone deposition.

The similarity between matrices shown by the lower jaws of giant ichthyosaurs, ossified tendons and osteoderms, can support speculations on biomechanical properties of the former (as already done by Horner, Woodward & Bailleul 2016 with the nasal of hadrosaur). For example, the largest element from Aust Cliff was suggested to belong to an animal in the size range of modern day blue whales (Lomax *et al.* 2018). Although the feeding strategy of these giant ichthyosaurs remains unknown, it is reasonable to assume that their large jaws were adapted to withstand significant stress associated with hunting and feeding underwater, similar to the feeding behavior of blue whales, which actively swallow thousands of liters of seawater (Goldbogen *et al.* 2007). Given the high tensile stress resistance of mineralized ossified tendons, it is possible that these large jaws were selected to withstand similar important stress, either during simple opening, as in baleen whales, or during possible shock-dealing behaviors, as observed in odontocetes like killer whales. At the same time the high amount of unmineralized fibers in the longitudinal axes would have provided a certain degree of flexibility on different planes of bending (Horner, Woodward & Bailleul 2016). The high rate of remodeling, typically related to bones experiencing strains, represents another factor supporting this hypothesis. Additionally it is possible to infer

that, like in ossified tendons, the presence of important soft tissue attachment, like muscles and connective tissue likely played an important role in the development of this peculiar histology (Organ & Adams 2005, Klein, Christian & Sander 2012; Horner, Woodward & Bailleul 2016). The occurrence of specializations toward buccal processing of large amounts of water is not isolated within Ichthyosauromorpha (Fang *et al.* 2023) and is to be expected within the evolutionary context of achievement of giant sizes in marine environments(Sander *et al.* 2021). Further studies and the examination of more complete specimens are necessary to test these ideas thoroughly.

Conclusions

Paleohistology can be a powerful tool for identifying the taxonomic affinity of fragmentary bone specimens, as demonstrated in previous studies on dinosaurs before (e.g., Garilli *et al.* 2009; Hurum *et al*. 2006). However, paleohistology can also be used to show that dinosaur-sized fragmentary bones do not belong to dinosaurs at all. Our study does that, rejecting Sauropodomorpha and Stegosauria as possible sources of the bone segments. Similarly, we reject any affinity with hypothetical giant Crurotarsi, Kannemeyeriiformes and plesiosaurs. We note similarities with secondarily aquatic tetrapods (Temnospondyli and large nothosaurs) but these groups are also dismissed due to significant differences and the less parsimonious claim that such large remains belong to these taxa. The observed similarities with temnospondyls and nothosaurs may be attributed to convergences in developmental strategies, possibly associated to the attainment of large sizes in aquatic environments.

On the other hand, the morphology-based Giant Ichthyosaur Hypothesis, which advocates the ichthyosaurian nature of the "dinosaur bone shafts" from the British Rhaetian deposits is supported by several osteo-histological observations found in the samples of Cuers and Lilstock ichthyosaurs and also in the benchmark, the holotype and other material of the giant *Shastasaurus sikanniensis* from Canada. We thus conclude that the Aust Cliff fragmentary samples indeed pertain to giant ichthyosaurs, as well as the cortex fragments from Bonenburg. WMNM P88133 and WMNM P-uncatalogued are recognized as a dermatocranial bone fragment, likely from the jaws, comparable in size to the British and French lower jaw fragments, suggesting the potential for similar discoveries of large-bodied ichthyosaurs in the Exter Formation of northern Germany.

Our study also provides important osteo-histological conclusions regarding the obscure Late Triassic giant ichthyosaurs.

The shared occurrence in several giant Late Triassic ichthyosaurs of a unique bone tissue, indicates a consistent ossification strategy in their lower jaws. This bone tissue is defined as PSFT, a kind of woven-parallel complex composed by a matrix of structural fibers and longitudinal osteons, resembling metaplastic bone, but clearly of periosteal origin. The occurrence of PSFT appears to be associated with closely spaced SGM, evidencing rhythmic

changes in bone formation, and ‘templating’ remodeling produced by secondary osteons developed primarily inside the primary ones.

These features may be apomorphic for a clade of giant ichthyosaurs and/or related to relevant biomechanical properties of their lower jaws. More comparable histological samples of ichthyosaurs and more complete specimens are needed to confirm these hypotheses.

Finally, our study shows that there are still novel bone tissue types to be discovered, restricted to a specific, extinct clade. PSFT apparently is extinct, and future work must be directed at the evolutionary, phylogenetic, and developmental dynamics associated with the nature of PSFT, its possible unrecognized presence in modern animals and the fossil record, and the reasons for its strong resemblance to the products of metaplastic ossification.

Acknowledgements

The authors would like to deeply thank Deborah Hutchinson and Roger Vaughan (BRSMG), Valentin Fischer (ULiège), Brandon Strelitzky and Don Brinkman (RTMP), and Achim Schwerman (WMNM) for granting access, sampling permission and assistance with photographic material and information related to the sampled specimens in their care. Olaf Dülfer and Pia Schucht (IGPB) are to be thanked for assistance and preparation of the thin sections. René-Paul Eustache (Combon, France) helped us with modifying the Leica polarizing microscope for circular polarization. We are grateful to Dorota Konietzko-Meier and Sudipta Kalita (University of Bonn), Peter Galton (University of Bridgeport), Dean Lomax (University of Manchester), and Paul De la Salle (The Etches Collection, England) for the informative and discussion. Many thanks to Andrzej Wolniewicz (Polish Accademy of Sciences) for informing us of the existence of von Huene (1912). Finally, we would like to thank the editor and reviewers for their work and useful comments for improving this manuscript.

References

Aaron J. E. 1980. Demineralization of bone in vivo and in vitro. *Metab. Bone Dis. Relat. Res.* 2S, 117– 125.

Aaron J. E. 2012. Periosteal sharpey's fibers: A novel bone matrix regulatory system. *Frontiers in Endocrinology* 3,1– 10. DOI 10.3389/fendo.2012.00098

Barth G., G. Pieńkowski, J. Zimmermann, M. Franz, and G. Kuhlmann. 2018. Palaeogeographical evolution of the Lower Jurassic: High-resolution biostratigraphy and sequence stratigraphy in the Central European Basin. *Geological Society Special Publication*, 469, 341– 369.

Benton M. J. 2015. *Vertebrate Palaeontology* (4th ed.). Wiley-Blackwell Ltd., Chichester, 506 pp.

Benton M. J., and P. S. Spencer. 1995. *Fossil Reptiles of Great Britain*, Springer Netherlands, Dordrecht, 386 pp.

Bianucci G., Lambert O., Urbina M., Merella M., Collareta A., Bennion R., Salas-Gismondi R., Benites-Palomino R., Post K., de Muizon C., Bosio C., Di Celma C., Malinverno E.,

718 Pierantoni P.P., Villa I. M. & Amson E. 2023. A heavyweight early whale pushes the
719 boundaries of vertebrate morphology. *Nature*. https://doi.org/10.1038/s41586-023-06381-1
720Bromage T. G., Goldman H. M., McFarlin S. C., Warshaw J., Boyde A., Riggs C. M. 2003.
721 Circularly polarized light standards for investigations of collagen fiber orientation in bone.
722 *The Anatomical Record (Part B: New Anat.)*, 274B, 157– 168.
723Buffrénil V. de and Quihlac A. 2021*a*. Bone Tissue Types: A Brief Account of Currently Used
724 Categories. 183–188. *In* de Buffrénil V., de Ricqlès A.J., Zylberberg L., & Padian K. (Eds.).
725 (2021). *Vertebrate Skeletal Histology and Paleohistology* (1st ed.). Boca Raton: CRC Press.
726 838 pp. https://doi.org/10.1201/9781351189590
727Buffrénil V. de and Quihlac A. 2021*b.* Bone Remodeling. 229– 241. *In* de Buffrénil V., de Ricqlès
728 A.J., Zylberberg L., & Padian K. (Eds.). (2021). *Vertebrate Skeletal Histology and*
729 *Paleohistology* (1st ed.). Boca Raton: CRC Press. 838 pp.
730 https://doi.org/10.1201/9781351189590
731Buffrénil V. de, Quihlac A. and Cubo J. 2021. Accretion Rate and Histological Features of Bone.
732 221– 227. *In* de Buffrénil V., de Ricqlès A.J., Zylberberg L., & Padian K. (Eds.). (2021).
733 *Vertebrate Skeletal Histology and Paleohistology* (1st ed.). Boca Raton: CRC Press. 838 pp.
734 https://doi.org/10.1201/9781351189590
735Buffrénil V. de, Zylberberg L. 2021. Remarks on Metaplastic Processes in the Skeleton. 247– 254.
736 *In* de Buffrénil V., de Ricqlès A.J., Zylberberg L., & Padian K. (Eds.). (2021). *Vertebrate*
737 *Skeletal Histology and Paleohistology* (1st ed.). Boca Raton: CRC Press. 838 pp.
738 https://doi.org/10.1201/9781351189590
739Callaway J. M., and J. A. Massare. 1989. *Shastasaurus altispinus* (Ichthyosauria, Shastasauridae)
740 from the Upper Triassic of the El Antimonio District, Northwestern Sonora, Mexico. *Journal*
741 *of Paleontology*, 63, 930– 939.
742Camp C. L. 1976. Vorläufige Mitteilung über große Ichthyosaurier aus der oberen Trias von
743 Nevada. *Sitzungsberichte der Akademie der Wissenschaften, mathematisch-*
744 *naturwissenschaftliche Klasse*, 185, 125– 134.
745Camp C. L. 1980. Large ichthyosaurs from the Upper Triassic of Nevada. *Palaeontographica, A*I,
746 170, 139– 200.
747Chinsamy A., Rubidge B.S. 1993. Dicynodont (Therapsida) bone histology: phylogenetic and
748 physiological implications. *Palaeontologia Africana*, 30, 97– 102.
749Cross S. R. R., Ivanovski N., Duffin C. J., Hildebrandt C., Parker A. and Benton M. J. 2018.
750 Microvertebrates from the basal Rhaetian Bone Bed (latest Triassic) at Aust Cliff, S.W.
751 England. *Proceedings of the Geologists' Association*, 129, 635– 653.
752Green J. L., Schweitzer M. H., Lamm E. 2010. Limb bone histology and growth in *Placerias*
753 *hesternus* (Therapsida: Amonodontia) from the Upper Triassic of North America.
754 *Palaeontology*, 53(2), 347– 364.
755Fang ZC., Li JL., Yan CB., Zou YR. Tian L., Zhao B. Benton M. J., Cheng L., Lai XL. 2023. First
756 filter feeding in the Early Triassic: cranial morphological convergence between *Hupehsuchus*
757 and baleen whales. *BMC Ecol Evo*, 23, 36. https://doi.org/10.1186/s12862-023-02143-9

Fischer V., Cappetta H.,Vincent P., Garcia G., Goolaerts S., Martin J. E., Roggero D. and Valentin X. 2014. Ichthyosaurs from the French Rhaetian indicate a severe turnover across the Triassic–Jurassic boundary. *Naturwissenschaften*, 101, 1027– 1040.

Galton, P. M. 2005. Bones of large dinosaurs (Prosauropoda and Stegosauria) from the Rhaetic Bone Bed (Upper Triassic) of Aust Cliff, southwest England. *Revue de Paleobiologie*, 24, 51–74.

Garilli V., Klein N., Buffetaut, E., Sander P. M., Pollina F., Galletti L., Cillari A. and Guzzetta D. 2009. First dinosaur bone from Sicily identified by histology and its paleobiogeographical implications. *Neues Jahrbuch für Geologie und Paläontologie - Abhandlungen*, 252, 207–216.

Goldbogen J.A., Calambokidis J., Oleson E., Potvin J., Pyenson N.D., Schorr G., Shadwick R.E. 2011. Mechanics, hydrodinamics and energetics of blue whale lunge feeding: efficiency dependence on krill density. *Journal of Experimental Biology*, 214, 131– 146. doi:10.1242/jeb.048157

Gravendyck J., Schobben M., Bachelier J. B., and Kürschner W. M. 2020. Macroecological patterns of the terrestrial vegetation history during the end-Triassic biotic crisis in the central European Basin: A palynological study of the Bonenburg section (NW-Germany) and its supra-regional implications. *Global and Planetary Change*, 194, 103286.

Gruntmeijer K., Konietzko-Meier D., Bodzioch A. 2016. Cranial bone histology of *Metoposaurus krasiejowensis* (Amphibia, Temnospondyli) from the Late Triassic of Poland. *PeerJ*, 4,e2685; DOI 10.7717/peerj.2685.

Gruntmeijer K., Bodzioch A., Konietzko-Meier D. 2021. Mandible histology in *Metoposaurus krasiejowensis* (Temnospondyli, Stereospondyli) from the Upper Triassic of Poland. *PeerJ*, 9,e12218; DOI 10.7717/peerj.12218.

Hogler J. A. 1992. Taphonomy and paleoecology of *Shonisaurus popularis* (Reptilia: Ichthyosauria). *Palaios*, 7,108– 117.

Horner J., Woodward H., Bailleul A. 2016. Mineralized tissues in dinosaurs interpreted as having formed through metaplasia: A preliminary evaluation. *C.R. Paleovol*, 15, 176– 196; DOI 10.1016/j.crpv.2015.01.006.

Huene, F. v. 1912. Der Unterkiefer eines riesigen Ichthyosauriers aus dem englischen Rhät. *Zentralblatt für Mineralogie, Geologie und Paläontologie*, 1912, 61– 63.

Hurum J.H., Bergan M., Müller R., Nystuen J.P. & Klein N. 2006. A Late Triassic dinosaur bone, offshore Norway. *Norwegian Journal of Geology*, 86, 117– 123.

Jones S.J., Boyde A. & Ali N.N. (1984) The resorption of biological and non-biological substrates by cultured avian and mammalian osteoclasts. *Anat Embryol*, 170, 247– 256.

Kelley N. P., and N. D. Pyenson. 2015. Evolutionary innovation and ecology in marine tetrapods from the Triassic to the Anthropocene. *Science*, 348, aaa3716; DOI 10.1126/science.aaa3716.

Kelley N. P., Irmis R. B., Depolo P. E., Noble P. J., Montague-Judd D., Little H., Blundell J., Rasmussen C., Percival L. M. E., Mather T. A. and Pyenson N. D. 2022. Grouping behavior in a Triassic marine apex predator. *Current Biology*, 32, 5398– 5405.e3.

Klein N. and Sander P. M. 2007. Bone histology and growth of the prosauropod *Plateosaurus engelhardti* MEYER, 1837 from the Norian bonebeds of Trossingen (Germany) and Frick (Switzerland). *Special Papers in Palaeontology*, 77, 169– 206.

Klein N. and Sander P. M. 2008. Ontogenetic stages in the long bone histology of sauropod dinosaurs. *Paleobiology*, 34, 247– 263.

Klein N., Christian A. and Sander P. M. 2012. Histology shows that elongated neck ribs in sauropod dinosaurs are ossified tendons. *Biology Letters*, 8 1032– 1035.

Klein N., Canoville A., and Houssaye A. 2019. Microstructure of vertebrae, ribs, and Gastralia of Triassic sauropterygians—New insights into the microanatomical processes involved in aquatic adaptations of marine reptiles. *Anatomical Record*, 302, 1770– 1791.

Konietzko-Meier D., Werner J. D., Wintrich T., and Sander P. M. 2019. A large temnospondyl humerus from the Rhaetian (Late Triassic) of Bonenburg (Westphalia, Germany) and its implications for temnospondyl extinction. *Journal of Iberian Geology*, 45, 287– 300.

Kosch B. F. 1990. A Revision of the skeletal reconstruction of *Shonisaurus popularis* (Reptilia : Ichthyosauria). *Journal of Vertebrate Paleontology*, 10, 512– 514.

Lacroix P. 1970. Recherches sur le remaniement interne des os. *Arch. Biol. (Liège)*, 81, 275– 304.

Lamm E.T. 2013. Preparation and sectioning of specimens; pp. 55–160. *In* K. Padian, and E.-T. Lamm (Eds.). *Bone Histology of Fossil Tetrapods*. *Advancing Methods, Analysis, and Interpretation.* University of California Press, Berkeley. 298 pp.

Lomax D., De la Salle R.P., Massare J. A., and Gallois R. 2018. A giant Late Triassic ichthyosaur from the UK and a reinterpretation of the Aust Cliff 'dinosaurian' bones. *PLoS ONE*, 13, 1– 16.

Maidment S. C., Norman D. B., Barrett P. M., and Upchurch P. 2008. Systematics and phylogeny of Stegosauria (Dinosauria: Ornithischia). *Journal of Systematic Paleontology*, 6, 367– 407.

McGowan C. and Motani R. 1999. A reinterpretation of the Upper Triassic ichthyosaur *Shonisaurus*. *Journal of Vertebrate Paleontology*, 19, 42– 49.

Mitchell J. 2017. *Cortical Bone Remodeling in Amniota - a Functional, Evolutionary and Comparative Perspective of Secondary Osteons*. PhD Dissertation, University of Bonn, Bonn, Germany. 225 pp.

Mitchell J. and Sander P. M. 2014. The three-front model: a developmental explanation of long bone diaphyseal histology of Sauropoda. *Biological Journal of the Linnean Society* 112, 765– 781.

Naish, D., and D. M. Martill. 2008. Dinosaurs of Great Britain and the role of the Geological Society of London in their discovery: Ornithischia. *Journal of the Geological Society* 165, 613– 623.

Nicholls, E. L., and M. Manabe. 2004. Giant ichthyosaurs of the Triassic-A new species of *Shonisaurus* from the Pardonet Formation (Norian, Late Triassic) of British Columbia. *Journal of Vertebrate Paleontology* 24, 838– 849.

Organ C., Adams J. 2005. The histology of ossified tendons in dinosaurs. *Journal of Vertebrate Paleontology*, 25(3), 602– 613.

Padian, K. and Woodward H. 2021. Archosauromorpha: Avemetatarsalia – dinosaurs and their relatives. 511– 549. *In* de Buffrénil V., de Ricqlès A.J., Zylberberg L., & Padian K. (Eds.). (2021). *Vertebrate Skeletal Histology and Paleohistology* (1st ed.). Boca Raton: CRC Press. 838 pp. DOI 10.1201/9781351189590

Perillo, M., Heijne J. 2023. Storms and bones: evidence for palaeocurrents in the Rhaetian bonebeds of Bonenburg (Germany).. *In* Alba D.M., Marigó J., Nacarino-Meneses, C., Villa A. (Eds.). Book of Abstracts of the 20th Annual Conference of the European Association of Vertebrate Palaeontologists, 26th June – 1st July 2023. *Palaeovertebrata*, Special Volume 1-2023: 208. DOI:10.18563/pv.eavp2023

Redelstorff R. and Sander P. M. 2009. Long and girdle bone histology of *Stegosaurus*: implications for growth and life history. Journal of Vertebrate Paleontology, 29, 1087– 1099.

Redelstorff R., P. M. Sander, and P. M. Galton. 2014. Unique bone histology in partial large bone shafts from Upper Triassic of Aust Cliff, England: An early independent experiment in gigantism. Acta Palaeontologica Polonica 59, 607– 615.

Reynolds S. H. 1946. The Aust section. *Cottswold Naturalists' Field Club, Proceedings*, 29, 29– 39.

Ricqlés A. de, Padian K. and Horner J. R. 2003. On the bone histology of some Triassic pseudosuchian archosaurs and related taxa. *Ann. de Paléont.*, 89, 67– 101.

Ricqlés A. de, Buffrénil V. de, Laurin M. 2021. Archosauromorpha: from early diapsids to archosaurs. 467– 483. *In* de Buffrénil V., de Ricqlès A. J., Zylberberg L., & Padian K. (Eds.). (2021). *Vertebrate Skeletal Histology and Paleohistology* (1st ed.). Boca Raton: CRC Press. 838 pp. DOI 10.1201/9781351189590

Sander P. M. 2000. Long bone histology of the Tendaguru sauropods: Implications for growth and biology. *Paleobiology*, 26, 466– 488.

Sander P. M. 2013. An evolutionary cascade model for sauropod dinosaur gigantism - overview, update and tests. *PLoS ONE*, 8,e78573 (23 pages).

Sander P. M. and Klein N. 2005. Developmental plasticity in the life history of a prosauropod dinosaur. *Science*, 310, 1800– 1802.

Sander P. M. and Andrassy P. 2006. Lines of arrested growth and long bone histology in Pleistocene large mammals from Germany: What do they tell us about dinosaur physiology? *Palaeontographica A*, 277, 143– 159.

Sander P. M., Klein N., Stein, K. and Wings, O. 2011. Sauropod bone histology and implications for sauropod biology. 276– 302. In Klein N., Remes, K., Gee, C. T. and Sander P. M. (eds). *Biology of the Sauropod Dinosaurs. Understanding the Life of Giants.* Indiana University Press, Bloomington, 344 pp.

Sander P. M., Griebeler E. M., Klein N., Juarbe J. V., Wintrich T., Revell L. J., and Schmitz L. 2021. Early giant reveals faster evolution of large body size in ichthyosaurs than in cetaceans. *Science*, 374:eabf5787 (15 pages).

876Sander P. M., Romero Pérez De Villar P., Furrer H., and Wintrich T. 2022. Giant Late Triassic
877 ichthyosaurs from the Kössen Formation of the Swiss Alps and their paleobiological
878 implications. *Journal of Vertebrate Paleontology*, 42, e2046017.
879Sander P. M., Wintrich T., Schwermann A. H., and Kindlimann R. 2016. Die paläontologische
880 Grabung in der Rhät-Lias-Tongrube der Fa. Lücking bei Warburg-Bonenburg (Kr. Höxter) im
881 Frühjahr 2015. *Geologie und Paläontologie in Westfalen* 88, 11– 37.
882Sander P. M., Wintrich T. 2021. Sauropterygia: Histology of Plesiosauria. 444– 455. *In* de
883 Buffrénil V., de Ricqlès A.J., Zylberberg L., & Padian K. (Eds.). (2021). *Vertebrate Skeletal*
884 *Histology and Paleohistology* (1st ed.). Boca Raton: CRC Press. 838 pp.
885 https://doi.org/10.1201/9781351189590
886Sanders, W. 1876. On certain large bones in Rhaetic beds at Aust Cliff, near Bristol. *Annual Report*
887 *of the Association for the Advancement of Science, Transactions of the Sections 1875*, 45, 88–
888 81
889Scheyer T. and Sander P. M. 2004. Histology of ankylosaur osteoderms: implications for
890 systematics and function. *Journal of Vertebrate Paleontology*, 24, 874– 893.
891Scheyer T. M., Syromyatnikova E. V., and Danilov I. G. 2017. Turtle shell bone and osteoderm
892 histology of Mesozoic and Cenozoic stem-trionychian Adocidae and Nanhsiungchelyidae
893 (Cryptodira: Adocusia) from Central Asia, Mongolia, and North America. *Fossil Record*, 20,
894 69– 85.
895Schobben M., Gravendyck J., Mangels F., Struck U., Bussert R., Kürschner W. M., Korn D., Sander
896 P. M, and Aberhan M. 2019. A comparative study of total organic carbon-δ13C signatures in
897 the Triassic-Jurassic transitional beds of the central European basin and western Tethys shelf
898 seas. *Newsletters on Stratigraphy*, 52, 461– 486.
899Skedros J. G., Sorenson S. M. and Jenson N. H. 2007. Are distributions of secondary osteon
900 variants useful for interpreting load history in mammalian bones? *Cells Tissues Organs*, 185,
901 285– 307.
902Stein K. and Sander P. M. 2009. Histological core drilling: a less destructive method for studying
903 bone histology. *In* Brown M.A., Kane J.F., and Parker W.G., (Eds.). Methods in fossil
904 preparation. *Proceedings of the First Annual Fossil Preparation and Collections Symposium*,
905 pp. 69-80.
906Stein K. and Prondvai E. 2014. Rethinking the nature of fibrolamellar bone: an integrative
907 biological revision of sauropod plexiform bone formation. *Biological Reviews of the*
908 *Cambridge Philosophical Society*, 89, 24– 47.
909Storrs, G. W. 1993. Terrestrial components of the Rhaetian (uppermost Triassic) Westbury
910 Formation of southwest Britain. *In* Spencer G. Lucas and Michael Morales (eds.), *The*
911 *Nonmarine Triassic, Transactions of the International Symposium and Field Trip on the*
912 *Nonmarine Triassic, New Mexico Museum of Natural History & Science Bulletin,* 3, 447–
913 451.
914Storrs, G. W. 1994. Fossil vertebrate faunas of the British Rhaetian (latest Triassic). *Zoological*
915 *Journal of the Linnean Society of London*, 112, 217– 259.

916Stutchbury, S. 1850. On a large cylindrical bone found by Mr. Thompson in the “Bone-bed” of Aust
917 Cliff, on the Severn. *Annual Report of the Association for the Advancement of Science,*
918 *Transactions of the Sections*, 19, 67.
919Surmik D., Słowiak-Morkovina J., Szczygielski T., Wojtyniak M., Środek D., Dulski M., Balin K.,
920 Krzykawski T., Pawlicki R. 2023. The first record of fossilized soft parts in ossified tendons
921 and implications for the understanding of tendon mineralization. *Zoological Journal of the*
922 *Linnean Society*, XX, 1– 20.
923van Oers R.F.M., Wang H. & Bacabac, R.G. 2015 Osteocyte Shape and Mechanical Loading. *Curr*
924 *Osteoporos Rep*, 13, 61–66. https://doi.org/10.1007/s11914-015-0256-1
925Vickaryous M. K., Meldrum G. and Russell A. P. 2015. Armored geckos: A histological
926 investigation of osteoderm development in *Tarentola* (Phyllodactylidae) and *Gekko*
927 (Gekkonidae) with comments on their regeneration and inferred function. *Journal of*
928 *Morphology*, 276, 1345– 1357.
929Wintrich T., Hayashi S., Houssaye A., Nakajima Y. and Sander P. M. 2017. A Triassic
930 plesiosaurian skeleton and bone histology inform on evolution of a unique body plan.
931 *Sciences Advances*, 3, e1701144, 1– 11.
932Woodward H. 2019. *Maiasaura* (dinosauria: Hadrosauridae) tibia osteohistology reveals non-
933 annual cortical vascular rings in young of the year. *Frontiers in Earth Science*, 7, 50. doi:
934 10.3389/feart.2019.00050
935Zylberberg L. 2021. Bone cells and organic matrix. 85–103. *In* de Buffrénil V., de Ricqlès A.J.,
936 Zylberberg L., & Padian K. (Eds.). (2021). *Vertebrate Skeletal Histology and Paleohistology*
937 (1st ed.). Boca Raton: CRC Press. 838 pp. https://doi.org/10.1201/9781351189590

Figure 1

Map of western and central European localities source of studied material.

Purple stars indicate the source of Rhaetian specimens of this study. Inset shows paleogeographic reconstruction of Europe and the Western Tethys in the Rhaetian (modified from Schobben *et al.* 2019). The red and green marks show the approximate position of investigated fossil localities in the shallow marine environments. Abbreviations: CEB, Central European Basin; RM, Rhenish Massif.

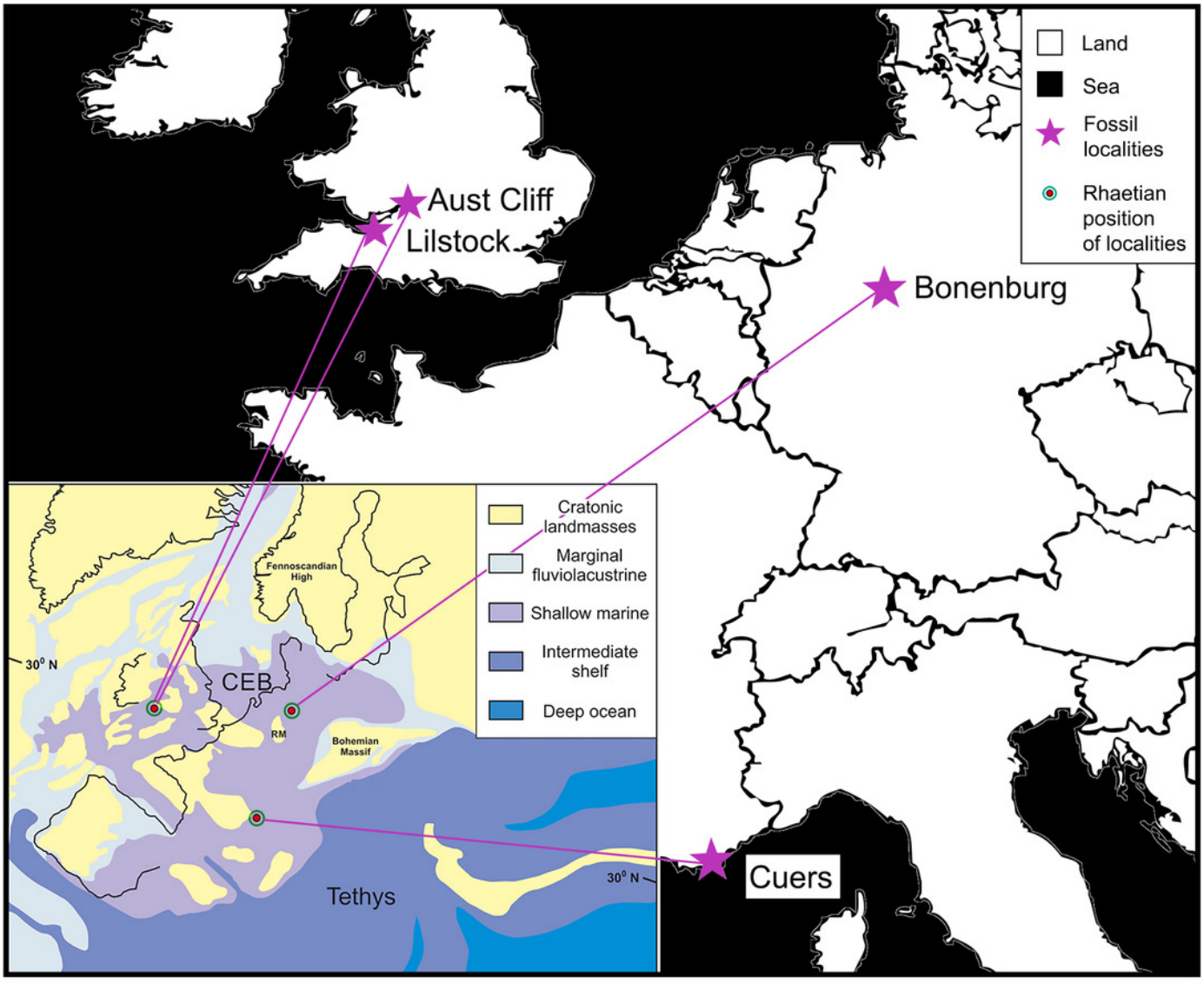

Figure 2

Main histological features of the giant ichthyosaurs lower jaws

(A) BRSMG-Cg-2488 seen in cross-polarized light (left) and with lambda filter added (right). The specimen shows a regular arrangement of layers of primary osteons showing internal resorption lines (concentric osteons), separated by SGMs, and high number of osteocyte lacunae. (B) Polarized light view of BRSMG-Cg-2488 showing the grid pattern of periosteal structural fibers that characterizes the matrix of all the samples. (C) BRSMG-Cg-2488 in circular polarized light revealing the somewhat/roughly helicoidal shape of the periosteal structural fibers and their interconnection within osteonal lamellar bone (top left). (D) Normal light view of the cross section of KULeuven PVL-1964 showing two primary osteons. The right one (dotted line) shows two concentric resorption lines and a poorly mineralized infilling. (E) Longitudinal section ofKULeuven PVL-1964 showing strands of unmineralized fibers (dark) running longitudinally in a herringbone pattern (green arrows) in direct light (left) and under lambda filter (right). (F) KULeuven PVL-1964 in normal light showing the irregular shape of osteocyte lacunae and the unmineralized fibers (green arrows). *Abbreviations*: Lb, lamellar bone; Po, primary osteon, PSF, periosteal structural fibers; Rl, resorption line Vc, vascular canal. Scale bars represent: 0,1 mm (A, B, D, E); 0,05 mm (C, F).

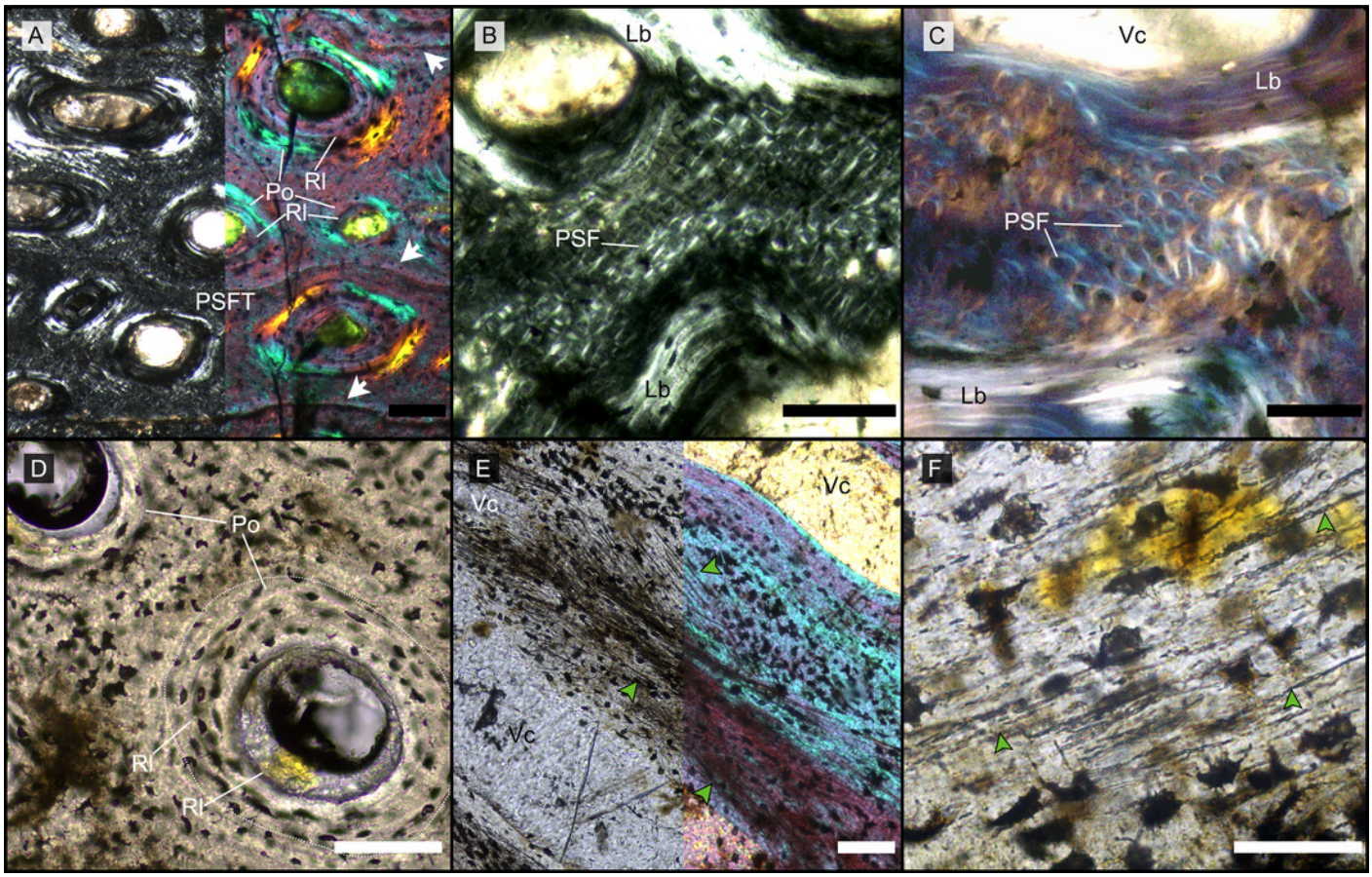
A
Po
Rl
Rl
PSFT
B
Lb
PSF
Lb
C
Vc
Lb
PSF
Lb
D
Po
Rl
Rl
E
Vc
Vc
Vc
F

Figure 3

Overview of composite micrographs of selected thin sections

The resorption front is indicated by a blue hatched line, a black dotted line indicates the boundary between rDC and tDC. (A) BRSMG-Cb-3869; (B) BRSMG-Cb-3870; (C) BRSMG-Cg-2488; (D) BRSMG-Cb-4063; (E) KULeuven PVL-1964. *Abbreviations*: DC, deep cortex; OC, outer cortex; rDC, regular deep cortex; RF, resorption front; tb, trabecular bone; tDC, templating deep cortex. All scale bars represent 2 mm.

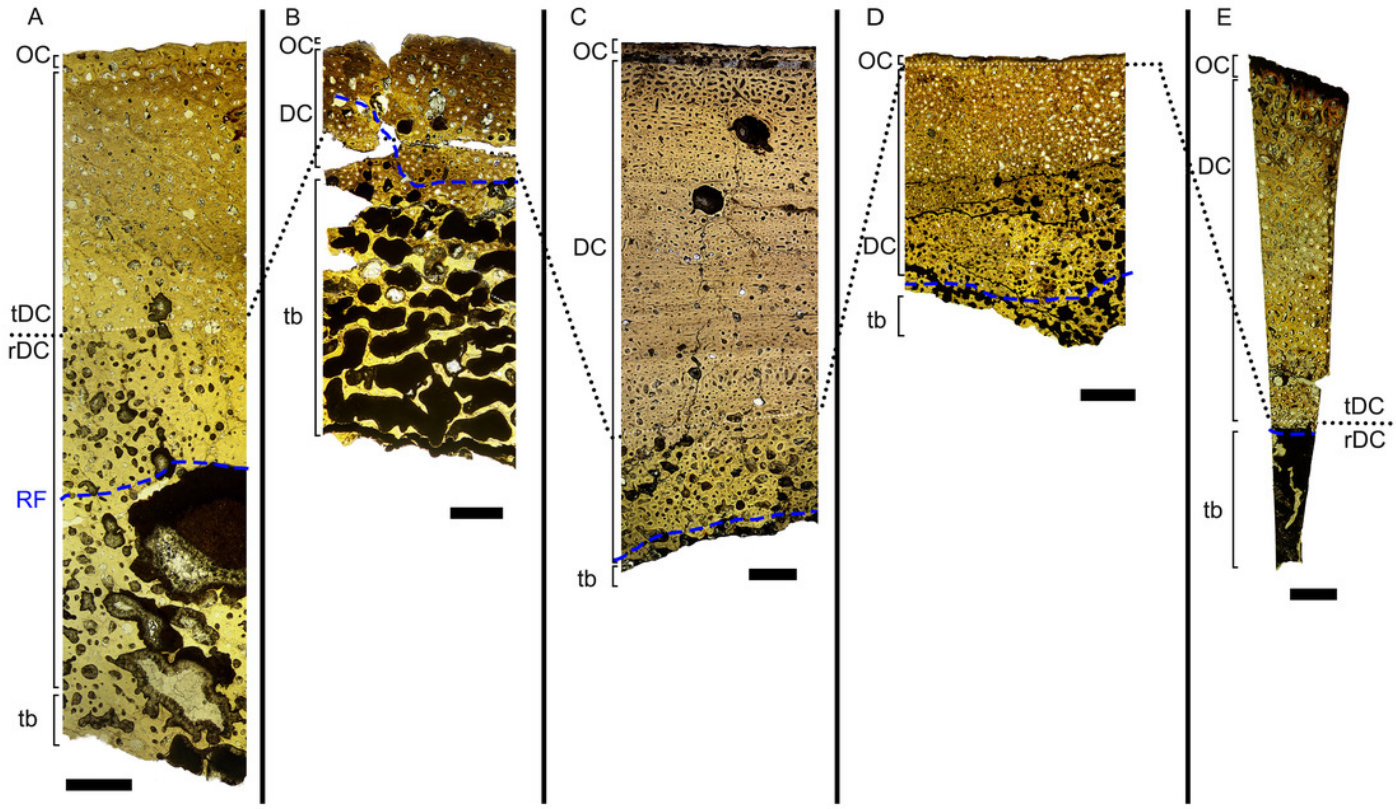

Figure 4

Features characterizing the areas identified as outer cortex, trabecular bone and deep cortex.

(A) Outer cortex of BRSMG-Cg-3870 in cross-polarized light (left) and with lambda filter added (right) showing primary tissue and ~~SGM~~. Secondary osteons are present on the outer edge of the bone and may interrupt the continuity of the SGM. The outer surface also shows diagenetic damage leading to the opening up of a secondary osteon. (B) BRSMG-Cb-3870 showing SGM (white arrows), an originally open periosteal canal and PSFT, under cross-polarized light and lambda filter. (C) Longitudinal section of KULeuven PVL-1964 in cross-polarized light (left) and with lambda filter added (right) revealing longitudinal vascularization. (D) Detail of trabecular bone of KULeuven PVL-1964 showing primary bone matrix of PSFT and primary osteons lined by secondary lamellar bone and cross-polarized light. (E-F) Nutrient canals in BRSMG-Cg-2488 (E) and BRSMG-Cb-3869 (F) in normal light. Both specimens show the presence of primary simple canals and SGM (white arrows) on the outer edge of the nutrient canal. Note the modified orientation of the SGM that follows the edge of the nutrient canal instead of being parallel to the outer surface of the bone. *Abbreviations*: Lb, lamellar bone; Nc, nutrient canal;oc, open vascular canal; PSFT, periosteal structural fibers tissue; So, secondary osteon. Scale bars represent: 0,1 mm (A-D); 2 mm (E, F).

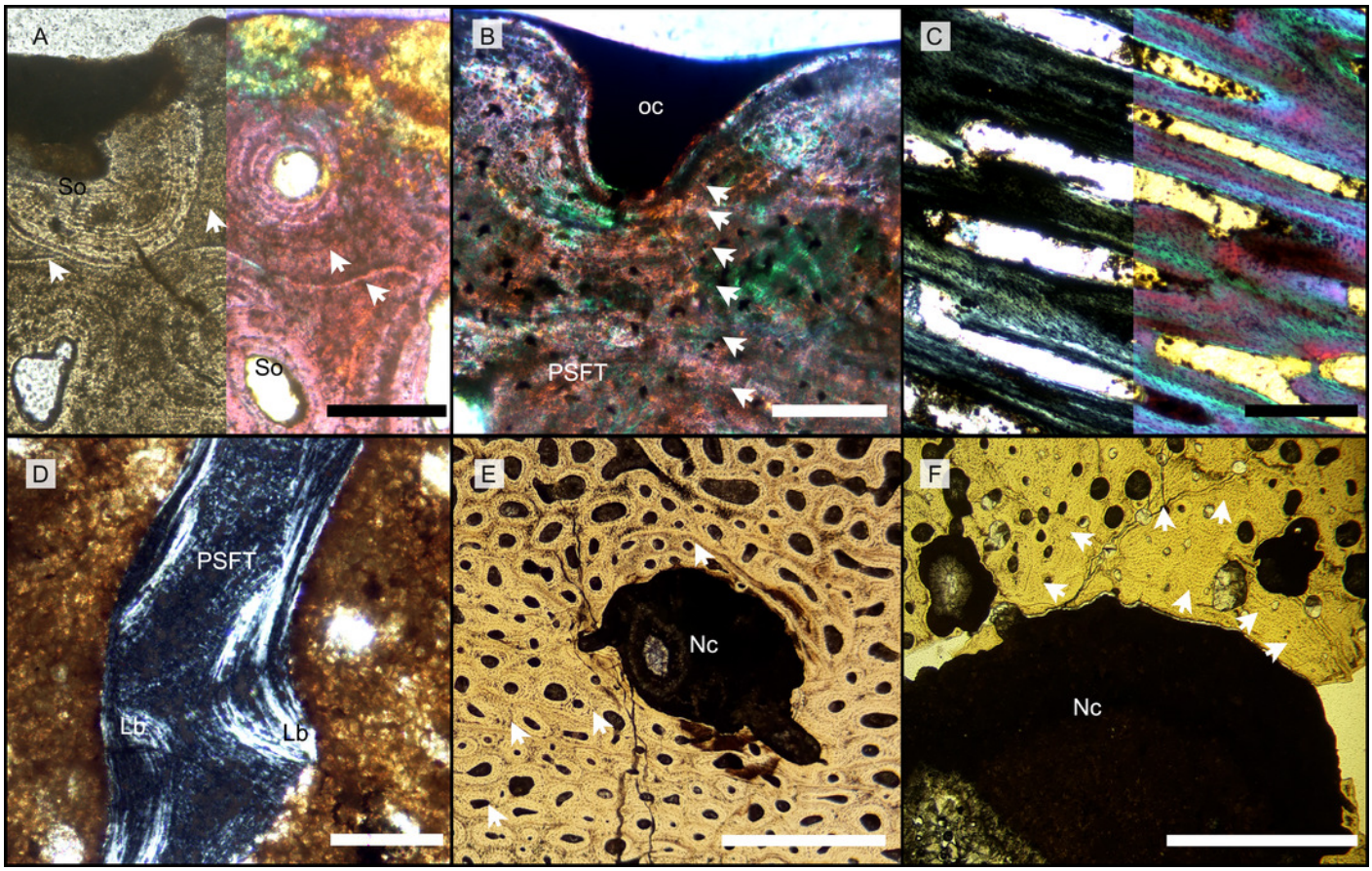
A
So
So
B
oc
PSFT
C
D
PSFT
Lb
Lb
E
Nc
F
Nc

Figure 5

Histology of the sample from the splenial of the *Shastasaurus sikanniensis* type specimen RTMP-1994-378-0002 from the middle Norian of British Columbia, Canada.

(A) Cross section of the splenial (dorsal at top), the highly cancellous structure is evident, as well as thelack of a dense outer cortex caused by taphonomic processes. (B) Close-up view of area indicated in A. Primary cortex with PSFT is preserved interstitially between secondary trabeculae. Left half of image is in cross-polarized light, right half in normal light. Note the dark stain of the bone tissue in the normal-light image. Post-mortem, pre-burial erosion of the bone surface t is evident from the truncation of the bone structure and cover by opaque sediment. (C-D) Close-up showing PSFT in cross-polarized light (C) and in circular polarized light (D). Note the helical arrangement of the fibers around a dark core. *Abbreviations*:PSF, periosteal structural fibers; PSFT, periosteal structural fibers tissue; RC, resorption cavity. Scale bars represent: 5,0 mm (A); 0,1 mm (B); 0,05 mm (C, D).

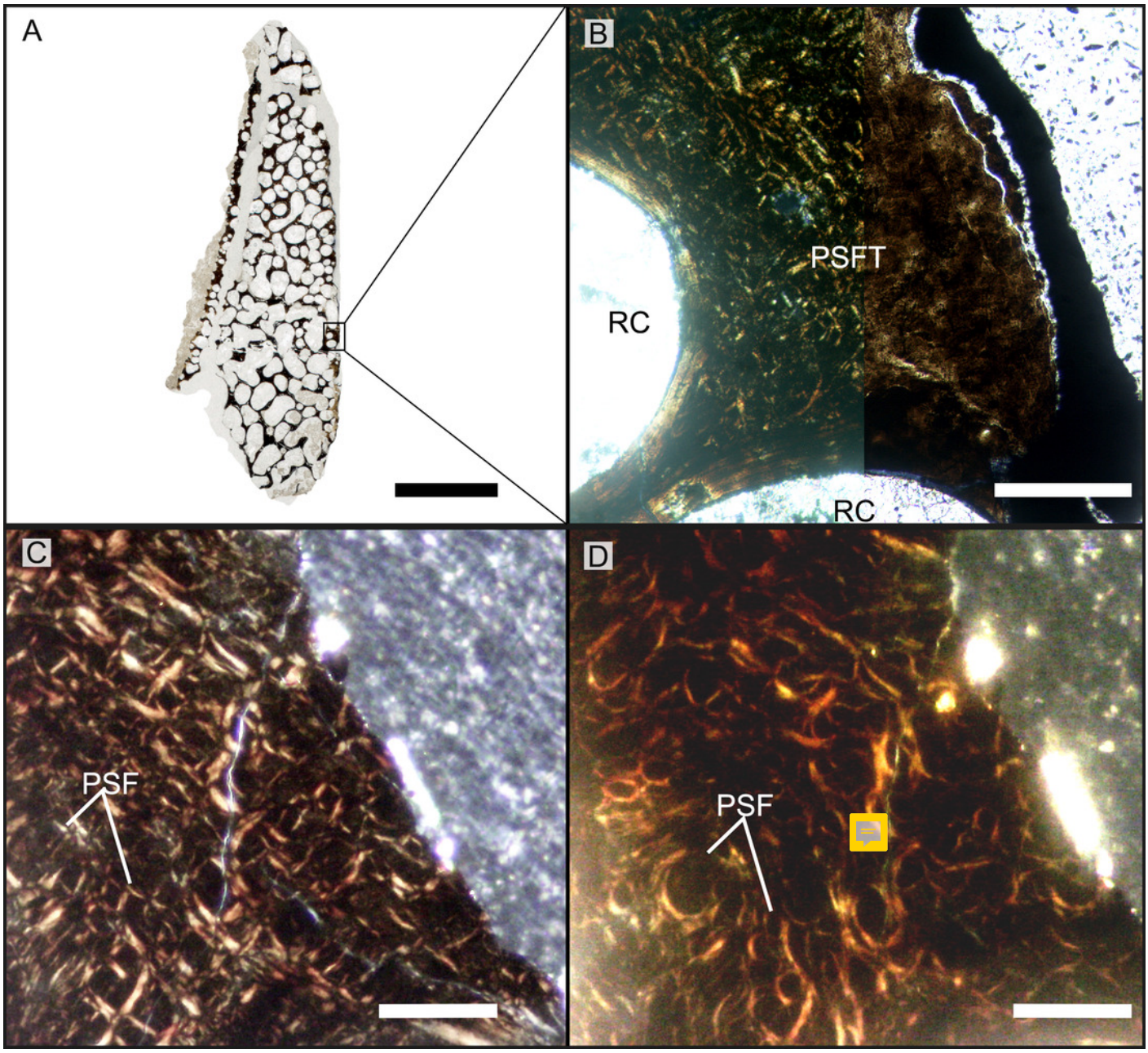
A
B
PSFT
RC
RC
C
PSF
D
PSF

Figure 6

Overview of WMNM P88133, the largest cortical bone fragment WMNM P88133 from the late Middle Rhaetian of Bonenburg, Germany.

Note the low curvature of the outer bone surface and the great thickness of the cortex, suggesting that the fragment derives from a very large bone. (A) Cross section showing a dark diagenetic seam staining the outer bone surface and the resorption front (blue dotted line). (B) Overview of the external cortex showing the characteristic, strictly longitudinal canals arranged in circumferential rows, open periosteal canals (partially hidden by the dark seam) and the numerous secondary osteons inside the primary ones and the concentric secondary osteons. The obliteration of the multiple parallel rows of SGM (white arrows) reveals the border between rDC and tDC (white dotted line). The tDC is characterized by essentially Haversian tissue. (C) Detail of the tDC, showing secondary osteons and primary matrix with periosteal structural fibers (left half of image cross-crossed polarized light left, right half circular polarized light). The periosteal structural fibers form a parallel SGM of alternating colors (white arrows). (D) Secondary osteon showing successive infilling of lamellar bone followed by woven or poorly mineralized bone (left side of image cross-polarized light with lambda filter, right side in cross-polarized light). (E) Longitudinal section seen in cross-polarized light with lambda filter showing unmineralized fiber strands (green arrows). *Abbreviations*: Cl, cementing line; HT Haversian tissue; Lb, lamellar bone; Oc: open vascular canal; rDC, regular deep cortex; RF, resorption front; tDC, templating deep cortex; So: Secondary osteon; Vc, vascular canal; Wb, woven bone. Scale bars represent: 2,0 cm (A); 1,0 mm (B); 0,1 mm (C-E).

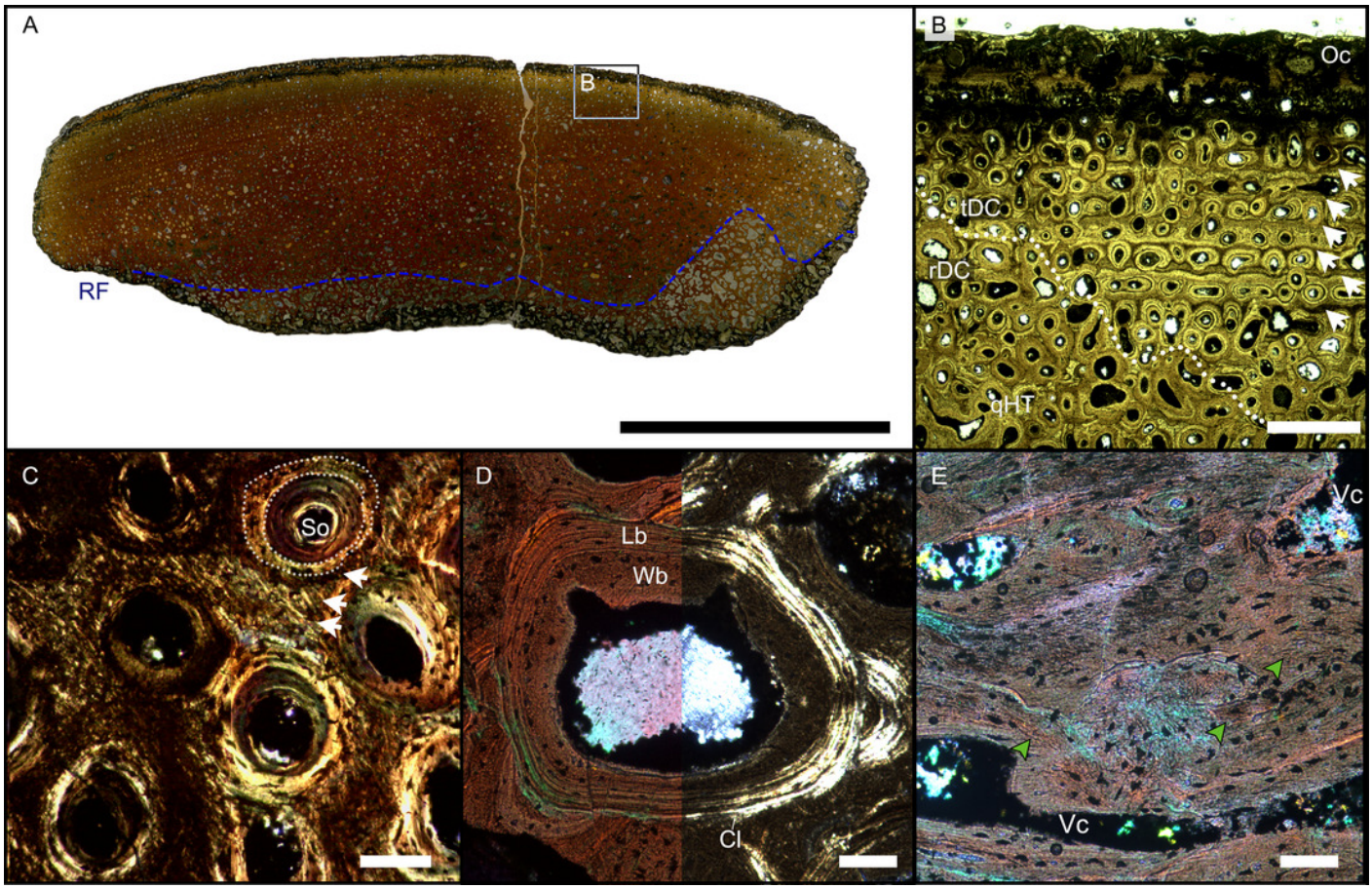
A
B
RF
B
Oc
tDC
rDC
qHT
C
So
D
Lb
Wb
Cl
E
Vc
Vc

Table 1(on next page)

List of specimens used in this study

1

Spec. No.	Locality	Age	Strat. Unit	Anatomy	Taxon	Reference	Samples	Sampling method	Plane of section	Thin section repository	Remarks
RTMP-1994-378-0002	Sikanni Chief River, British Columbia,	middle Norian	Pardonet Formation	surangular, splenial	*S. sikanniensis*	Nicholls & Manabe 2004	2	cut	cross	IGPB	holotype
BRSMG-Cg-2488 R-101	Lilstock, UK	Rhaetian	Top of Westbury Mudstone Formation	surangular	Shastasauridae indet.	Lomax et al. 2018	1	core	cross	BRSMG	
BRSMG-Cb-3869, 3870, 4063	Aust Cliff, UK	Rhaetian	Rhaetic bonebed at base of Westbury	surangular	Shastasauridae indet.	Galton 2005; Redelstorff et al. 2014; Lomax et al.	3	core	cross	BRSMG	
KULeuven PVL-1964	Autun, France	Rhaetian	Grès à Avicula contorta, Grès Blonds Formation	surangular	Shastasauridae indet.	Fischer et al. 2014, Lomax et al. 2018	2	core, cut	cross and long	IGPB	
WMNM P-uncatalogued	Bonenburg, Germany	late middle Rhaetian	Exter Formation	cortical fragment	Tetrapoda indet.	Sander et al. 2016	1	cut	cross	IGPB	
WMNM P88130,..,P88144	Bonenburg, Germany	late middle Rhaetian	Exter Formation	15 cortical fragments	Tetrapoda indet.	Sander et al. 2016	14	cut	cross and long	IGPB	

Table 2(on next page)

Comparison of the osteohistological features across our study sample and other Late Triassic taxa

The results here summarized are based on literature research and, when available, on authors observation of the samples in the GIPB histology collection. *Abbreviations*: WPC, woven-parallel complex; PSFT, periosteal structural fiber tissue.

Groups considered in this study	Source of histological samples	Main bone organization	Vascularization rate	Vascular organization	Cyclical structures	Periosteal remodeling strategy	Relative remodeling rate	Abbundant concentric osteons	Main references
Giant Rhaetian ichthyosaurs	Lower jaws	WPC with PSFT	High	Longitudinal	SGMs	Template + diffused	High	Yes	This study
British bone segments	Lower jaws(?)	WPC with PSFT	High	Longitudinal	SGMs	Template + diffused	High	Yes	Redelstorff, Sander & Galton (2014), this study
S. sikanniensis	Splenial and surangular	WPC with PSFT	High	Longitudinal	Not preserved	Not preserved	Not preserved	Not preserved	This study
Bonenburg cortical fragments	Unidentified cortices	WPC with PSFT	High	Longitudinal	SGMs	Template + diffused	High	Yes	This study
Sauropodomorpha	Long bones	WPC (fibrolamellar)	Moderate to high	Plexiform/laminar	LAGs	Organized front	Moderate to high	Not observed or reported	Klein & Sander (2007); Mitchell & Sander (2014)
Stegosauria	Long bones	WPC	Moderate	Longitudinal	LAGs	Scattered front	Moderate to high	Not reported	Redelstorff & Sander (2009); Padian & Woodward (2021)
Rauisuchia - Slow growth	Long bones	Lamellar-Zonal + WPC	Low	Laminar/subplexiform	Annuli+LAGs	Scattered	Low	Not reported	de Ricqlès et al. (2003); de Buffrénil et al. (2021)
Rauisuchia - Fast growth	Long bones	WPC	Moderate to high	Laminar/subplexiform	Annuli	Scattered	Low	Not reported	Klein et al. (2017); de Buffrénil et al. (2021)
Phytosauria	Long bones	Lamellar-Zonal	Low	Longitudinal	Annuli+LAGs	Scattered front	Low	Not reported	de Ricqlès, Padian & Horner (2003); ; Ricqlés, Buffrénil & Laurin (2021)
Dicynodontia	Long bones	WPC	Moderate to high	Longitudinal	SGMs	Scattered and unorganized		Not reported	Chinsamy & Rubidge (1993); Green, Schweitzer & Lamm (2010)
Plesiosauria	Long bones	WPC	Moderate to high	Longitudinal+radial	SGMs	Template + front	High	Yes (?)	Wintrich *et al* . (2017); Sander & Wintrich (2021)
large Nothosauria	Ribs	WPC+PSFs	Moderate to high	Longitudinal+radial	LAGs	Absence	Low	Not reported	Klein, Canoville & Houssaye. (2019)
Temnospondyili	Lower jaws, long bones	Lamellar-Zonal+PSFs/ISFs	Low to moderate	Longitudinal+plexiform	Annuli+LAGs	Template	Low to moderate	Not reported	Konietzko-Meier et al. (2019); Gruntmejer, Bodzioch & Konietzko-Meier (2021)